Formation and Immunological Properties of Myelin in the Central Nervous System

Dissertation
zur
Erlangung der naturwissenschaftlichen Doktorwürde
(Dr. sc. nat.)

vorgelegt der
Mathematisch-naturwissenschaftlichen Fakultät
der
Universität Zürich
von

Anna Bettina Sobottka
aus
Deutschland

Promotionskomitee
Prof. Dr. Dr. Adriano Aguzzi
Prof. Dr. Burkhard Becher
Prof. Dr. Norbert Goebels
Prof. Dr. Sebastian Jessberger

Zürich, 2010

Disclaimer

This thesis was based upon and partly adapted from the following publications:

- Sobottka B, Harrer MD, Ziegler U, Fischer K, Wiendl H, Hünig T, Becher B, Goebels N. Collateral bystander damage by myelin-directed CD8+ T cells causes axonal loss. *Am J Pathol.* **2009** Sep;175(3):1160-6

- Sobottka B, Ziegler U, Kaech A, Becher B, Goebels N. CNS live imaging implies a new mechanism of myelination: The liquid croissant model (manuscript in preparation)

Table of contents

Summary

Permanent disability of patients suffering from central nervous system (CNS) inflammation such as multiple sclerosis (MS), the most common chronic inflammatory disorder of the CNS, originates mainly from demyelination and axonal damage.

Among other immune mediators, autoaggressive, cytotoxic CD8+ T cells have received increasing attention over the past years in MS pathogenesis. Yet, it has remained elusive whether axonal injury is the result of a CD8+ T cell-targeted hit against the axon itself or the consequence of an attack against the myelin structure. To address this issue, we traced the interaction of autoaggressive CD8+ T cells with living CNS tissue preserved in organotypic cerebellar brain slices by continuous confocal imaging. We restricted cognate antigen expression to the cytosol of oligodendrocytes to exclude its direct presentation by other CNS cell types. Using this model system of CNS inflammation, we visualized that axonal loss can be the consequence from "collateral bystander damage" by autoaggressive CD8+ T cells, targeting their cognate antigen processed and presented by oligodendrocytes.

In a similar experimental set-up, we investigated myelin formation in the CNS. In general, its understanding appears closely connected with the regenerative process of remyelination after pathological demyelination like in MS and represents a challenging problem in view of the concerns towards the currently most accepted myelination model. We therefore performed a comprehensive live imaging, light and electron microscopy study of myelin formation in mouse CNS. Based on our data, we suggest a new mechanism of myelination, “The liquid croissant model”. Our new myelination concept does not only resolve the current, most suspected concerns and plausibly explains previous observations but attributes a new role to the axon, the

guidance of myelination. We believe that our model reshapes the current understanding of myelination and may help to explain myelination deficits in remyelination and axonopathies.

Zusammenfassung

Entzündungen im zentralen Nervensystem (ZNS), unter denen die Multiple Sklerose (MS) am häufigsten vorkommt, sind oft mit permanenter, neurologischer Behinderung verbunden. Diese kann oft auf den Verlust von Myelin (Demyelinisierung) und Axonen zurückgeführt werden.

Neben anderen in der MS Pathogenese beteiligten Immunmediatoren sind autoagressive, zytotoxische CD8+ T Zellen in den letzten Jahren in den Mittelpunkt gerückt. Dennoch blieb es unklar, ob der axonale Schaden direkt durch CD8+ T Zellen entstehen könne oder ob er aus deren Angriff auf das Myelin resultiere. Um dies aufzuklären, haben wir mittels konfokaler Livemikroskopie autoagressive CD8+ T Zellen in organotypischen ZNS Gewebeschnittkulturen beobachtet. Dabei haben wir die Expression des kognitiven Antigens auf das Zytosol von Oligodendrozyten beschränkt, um eine direkte Präsentation durch Axone auszuschließen. Anhand dieses ZNS-Entzündungsmodells konnten wir zeigen, das Antigenpräsentation durch Oligodendrozyten einen axonalen Kollateralschaden durch CD8+ T Zellen hervorrufen kann.

Anhand eines ähnlichen experimentellen Modells, haben wir die Entstehung des Myelins im ZNS untersucht. Generell ist das Verständnis der Myelinisierung nicht nur eng mit dem der Remyelinisierung nach einer pathologischen Demyelinisierung wie z. B. in der MS verknüpft, sondern stellt auch ein interessantes Problem in Anbetracht der Zweifel am jetzigen Myelinisierungsmodell dar. Wir haben daher eine umfassende live-, licht- und elektronen-mikroskopische Studie der Myelinisierung im ZNS der Maus durchgeführt. Unseren Ergebnissen zufolge haben wir eine neue Myelinisierungshypothese formuliert, das „flüssige Croissant-Modell“. Damit können nicht nur die größten Zweifel der bisherigen Myeliniserungstheorie gelöst und vorherige Beobachtungen erklärt werden, sondern das Axon selbst erhält eine neue

Aufgabe, indem es die Myeliniserung lenkt, was eine wesentliche Rolle bei Defiziten während der Remyelinisierung oder in Axonopathien spielen könnte.

1 Introduction

1.1 Overview

Given the still limited treatment options in many neurological diseases, the study of (patho)physiological processes in the central nervous system (CNS) is of major importance. In this regard, only investigation in real time with resolution in the micrometer range allows answering certain research questions but has been challenging to fulfill, especially in the CNS. We have therefore established high-resolution confocal live imaging of CNS tissue by employing organotypic cerebellar slice cultures (OCS) as a model system, where the CNS cytoarchitecture is preserved in-vitro and where certain conditions can be applied in a defined manner. In view of the high portion of patients suffering from multiple sclerosis (MS), where long-term neurological deficits appear to result from demyelination and axonal damage, we (1) established a model of CNS inflammation, where CD8+ T cells can be observed in real-time to destroy myelinated axons and (2) studied the process of myelin formation in its dynamic phase, which may help to understand the failure of regenerative processes, such as remyelination also seen in MS.

1.2 Clinical signs and pathogenesis of Multiple Sclerosis

More than 100 years ago, Charcot and others described MS by its clinical symptoms and pathological characteristics. Nowadays, MS is the most common inflammatory disorder of the CNS, thought to be caused by an immune response against components of myelin. It appears to affect genetically prone individuals most likely after exposure to an environmental trigger. Its prevalence is the highest in civilized countries the furthest away from the equator, like northern Europe, southern Australia, and North America and it affects patients in their second or third decade in life with a female predominance of 2:1 [1].

Clinically, MS shows in most cases an alternation of relapses (episodes of demyelination and inflammation) followed by remissions (remyelination and plasticity), and is thus referred to as relapsing-remitting MS. During the relapse phase the neurological symptoms depend on the site of lesion but may include sensory loss, weakness in leg muscles, speech difficulties, loss of coordination and dizziness. The majority of the relapse-remitting MS patients will experience eventually a secondary progressive disorder with continuous neurological deficits lacking any remission phase, most likely due to less effective remyelination over time [2]. In contrast, some patients develop primary progressive MS without any remission from the start of the disease. These patients often suffer from an upper motor-neuron syndrome of the legs that worsens gradually and becomes combined with various other concomitant symptoms [1]. The typical diagnostic process consists of the clinical criteria together with (1) assessment of the Expanded Disability Status Scale (EDSS), (2) visual and sensory evoked potentials [3],(3) cerebrospinal fluid (CSF) analysis, where an intrathecal synthesis of immunoglobulins (Ig) can often be observed with oligoclonal bands representing IgGs and (4).magnetic resonance imaging (MRI) with multifocal lesions especially in the periventricular white matter, brain stem, cerebellum and spinal cord.

Yet, the exact pathophysiological causes for disease's initiation and perpetuation are far from being understood. Detailed histological studies of MS brain tissue indicate that different disease mechanisms may prevail in individual subgroups of MS patients [4] and that the disease consists of an inflammatory and degenerative phase [5]. In general, the pathological hallmarks of acute MS lesions contain members of both innate and adaptive immunity (see later) and feature perivascular lymphocyte cell infiltrates, parenchymal edema, demyelinating plaques with loss of oligodendrocytes (OLG), axonal damage, myelin-laden macrophages, hypertrophic astrocytes in

brain and spinal cord [6]. However, it has remained enigmatic, which of these immune components are the key players in MS pathophysiology.

1.3 The immune system with an emphasis on T cell-mediated autoimmunity

Cell-mediated events in the immunopathology of MS development are clearly important and have been shown to play a crucial role also in other organ-specific autoimmune diseases [7]. As one part of this thesis focused on the role of CD8+ T cells in CNS inflammation, I will briefly discuss the workings on the immune system relevant to understand T cell self-tolerance, activation and autoimmunity.

1.3.1 The immune system

Virtually every organism comes with a system that protects it from pathogenic invasion of foreign molecules. In case of higher vertebrates the immune system exists of two branches, termed the innate and adaptive immune systems [8]. In concert, they defend the organism but have different tasks assigned: Whereas innate immunity responds rapidly to antigens at the expense of specificity, acquired or adaptive immunity is specific and generates immunological memory.

1.3.2 Innate immunity

The innate immune system [9] comprises natural killer (NK) cells, γ/δ T cells, polymorphonuclear leukocytes (PMNs) and professional antigen presenting cells (APCs) like monocytes/ macrophages and dendritic cells (DCs). These defend the host against pathogens by recognizing specific molecular components of invading micro-organisms, known as pathogen-associated molecular patterns (PAMP). The discrimination of self versus non-self relies on the fact that PAMPs are absent in the host but are indispensable of the invading pathogen. To recognize PAMPs, innate immune cells hold germ-line encoded receptors called pattern recognition

receptors (PRR) [10]. PRRs can be either in a soluble form like mannose-binding lectins (MBL) [11], C-reactive protein (CRP) [12] and complement [13] or they can be membrane bound receptors like the scavenger receptors [14] and the key structures of recognition, the toll-like receptors (TLR) [15], usually present on APCs. The different TLRs respond to bacteria, viruses, fungi or protozoa with increased phagocytic activity, release of inflammatory mediators, production of reactive oxygen species and secretion of cytokines. The secreted cytokine profile can crucially steer the subsequent adaptive immune response (see later).

1.3.3 Adaptive immunity

T and B lymphocytes are the cells of the adaptive immune system that mediate either humoral (B cells) or cellular (T cells) immunity. They recognize foreign structures through highly specific receptors, generated by somatic recombination. Their ability to form immunological memory upon antigen encounter allows a faster response, with greater reactivity, upon a second antigen hit. They both derive from bone marrow hematopoietic stem cells but follow different paths for their "education" in distinguishing self and non-self.

1.3.4 Formation of T cell self-tolerance

In the case of T cells, they migrate to the thymus, where they rearrange the alpha and beta chains of the T cell receptor (TCR) during maturation. In order to recognize the body's own cells in the context of antigens, T cells become selected during a process called *central tolerance* [16]: (1) to ensure the recognition of self-MHC, only the T cells that recognize self-MHC molecules expressed on thymic epithelial cells (TECs) are positively selected, non-recognition results in apoptosis. This part of selection is referred to as *self-restriction* by *positive-selection*. (2) In a second step termed *negative selection*, T cells "learn" to recognize foreign antigen. Here,

medullary TECs or specialized DCs express many tissue-restricted auto-antigens on self-MHC [17]. Highly self-affine T cells become largely deleted, while receptor editing also occurs [18]. T cells with a low affinity response survive and are released into the periphery.

Although the mechanism of *central tolerance* is aimed at the deletion of self-recognizing T cells, it is not faultless. As a result, next to T cells that survived both *positive* and *negative selection*, potentially auto-reactive lymphocytes are released and may circulate in a naïve stage in the body's blood and lymph streams. Therefore, to ensure a healthy immune system, several control mechanisms exist that are collectively referred to as *peripheral tolerance*: (1) potentially harmful cells are rendered anergic (functionally unresponsiveness) or become (2) deleted (apoptotic cell death) or (3) are suppressed by regulatory T cells (T_{regs}) that were identified in CD25+ depletion experiments [19,20]. That these mechanisms work and that auto-reactive and protective T cells coexist was demonstrated in similar numbers of myelin-reactive CD4+ T cells in the blood and CSF of MS patients and healthy individuals [21], suggesting that environmental factors contribute to the development of autoimmunity (see below).

1.3.5 T cell activation

T lymphocytes are distinguished according to their TCR co-receptors in CD4+ and CD8+ T cells. They recognize processed peptide antigens only when presented on self-MHC molecules [22] in the following manner: CD8+ T cells react to peptides bound on MHC class I molecules, expressed by virtually all nucleated cells of the body. MHC class I molecules present cell endogenous peptides, which is not only important for self-recognition but also to present intracellular pathogens (i.e. viruses). In contrast, CD4+ T cells recognize exogenous peptides presented by MHC class II molecules, expressed only by professional APCs. In a link between innate and adaptive immunity, APCs activate T cells in a process called *priming* by providing: a

suitable MHC/peptide complex interacting with the TCR (signal 1) and an additional co-stimulatory signal like CD80 or CD86, which interacts with the T cell's CD28 molecule (signal 2). Depending on the co-stimulatory molecules of APCs that interact with their respective receptors on T cell, the signal is either stimulatory or inhibitory. Activation of T cells without co-stimulation may lead to T cell anergy or deletion.

The cytokine pattern secreted by APCs upon T cell encounter (signal 3) essentially influences the outcome of the T cell immune response. Consequently, CD4+ T cells, also known as helper T (T_h) cells, can differentiate into different subtypes, which in turn produce cytokines affecting the overall immune response. For example, type 1 helper T (T_h1) cells are involved in cell-mediated immunity by producing pro-inflammatory cytokines like interferon-γ (IFN-γ), interleukin (IL-) 2 and tumor necrosis factor (TNF-) β, which can activate macrophages or CD8+ T cells [23]. In contrast, type 2 helper T (T_h2) cells are characterized by the production of IL-4, IL-5, IL-9, and IL-13 and take part in a humoral immune response. In addition to this classical paradigm, CD4+ T cells can be polarized depending on the cytokine milieu into for example T_h17 cells [24], T_h3 cells or transforming growth factor (TGF)-β induced regulatory T cells (T_{regs}) [25].

After CD8+ T cells received their activating signals from professional APCs in analogy to CD4+ T cells [26], they turn into cytotoxic T lymphocytes (CTLs) that induce apoptosis of their target cells by the tumor necrosis factor α (TNFα) member the Fas-ligand or by exocytosis of cytoplasmic granule toxins. To the latter belong the membrane-disrupting protein perforin and serine proteases, so called granzymes [27]. For a schematic view on CD8+ T cell mediated cell death of target cells see Fig. 1.

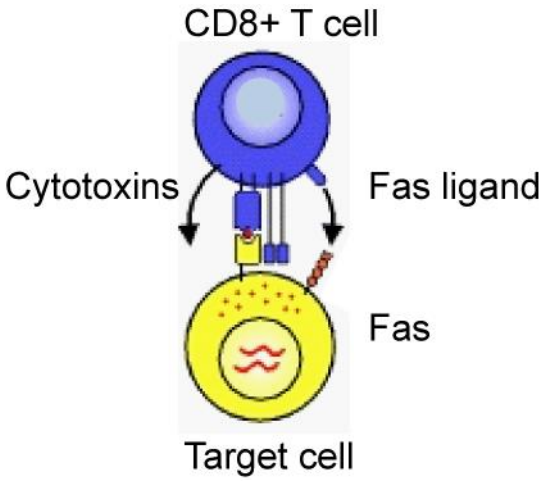

Fig. 1 **Recognition and induced target cell death by a cytotoxic CD8+ T lymphocyte**. After recognition of the target cell via MHC class I/TCR, an activated, cytotoxic CD8+ T cell (blue) mediates target cell (yellow) death by exocytosis of the cytotoxins perforin and granzymes or by Fas ligand secretion (adapted to Janeway, Travers, 2001).

1.3.6 T cell-mediated autoimmunity

If the crucial process of T cell "education" in the thymus (see above) fails and releases self-reactive T cells that get beyond peripheral control, immunological tolerance is lost, which can result in autoimmune diseases. Nowadays, autoimmune diseases are major causes of morbidity and mortality and are still difficult or impossible to cure [28]. The clinical challenge relies in the nature of the disease as the cause of the immune response –self antigens – cannot be eliminated. The reasons for loss of immunological tolerance are not entirely clear yet but appear to be a combination of genetic polymorphisms, acquired environmental triggers and stochastic events. Up to now, they have been best described for CD4+ T cells: (1) most well-known became the contribution of genetic factors when *AIRE* was identified as the mutated gene in the autoimmune polyendocrine syndrome -1 (APS-1) [29]. Subsequent studies in *AIRE* knock-out mouse models

revealed that *AIRE* protein is responsible for the thymic expression of self-antigens that are elsewise expressed only in peripheral tissue [30]. Consequently, the absence of thymic self-antigen expression lets T cells escape *negative selection* with an eventual attack of the body's own tissue [31]; (2) Despite the broad self-peptide presentation in the thymus (see above), not all possible self-antigens may be expressed or may be presented at a level too low to activate T cells [32], resulting in the release of self-reactive T cells; (3) Although experimental and clinical models fall short in explaining the underlying mechanisms of molecular mimicry, at least for MS and type I diabetes mellitus it has been hypothesized. There, infectious agents (like viruses) are supposed to share antigenic structures with the host's own tissue resulting in a cross-reactive host's immune response against self-antigens. However, as infections are common and autoimmunity is not, further research is necessary to understand the exact pathways [33]; (4) an imbalance of cytokines has been demonstrated in various animal models to be implicated in T cell mediated autoimmune pathogenesis [34].

1.4 The pathogenic role of CD8+ T cells in Multiple Sclerosis

Activated auto-reactive T cells were assumed to play a key role in MS pathogenesis as was suggested by the association between MHC class II alleles and MS [35,36] as well as findings in experimental autoimmune encephalomyelitis (EAE) [37]. In support, MBP-specific CD4+ T cells were shown to contribute to axonal damage when employing organotypic slice cultures of murine hippocampus [38,39]. In MS patients, however, the specific depletion of CD4+ T cells could reduce neither the relapse rate nor the inflammatory status [40].

Thus, the almost exclusive focus on CD4+ T cells in MS autoimmune research turned out to be oversimplified and too imbalanced. Recently, compelling evidence pointed out the pathogenic

importance of auto-aggressive, cytotoxic CD8+ T cells in MS [41]. For example, histological investigations on MS brain tissue revealed that CD8+ T cells outnumber CD4+ T cells within demyelinating CNS lesions [42] and that they closely interact with demyelinated axons [43]. Furthermore, CD8+ T cells were found clonally expanded in the CSF, in the blood and in CNS lesions of MS patients [42,44]. In addition, CD8+ T cells from MS patients showed a higher frequency in CNS-antigen specificity in-vitro when compared to healthy controls [45] Finally, depletion of CD4+ T cells in MS patients showed no improvement in disease, whereas depletion of both CD4+ and CD8+ T cells was beneficial [46].

Experimental set-ups provided functional evidence on CD8+ T cell-mediated lysis of human leukocyte antigen (HLA)-matched OLG [47] and transsection of dissociated single neurons [48]. In support, in-vivo studies reported CNS injury after injecting myelin-specific CD8+ T cells either by using CD8-mediated EAE [49,50] or by employing novel approaches, where mice selectively express a neo-self antigen in OLG [51,52]. In both cases, the CD8+ T cell-induced demyelinating disease resembled certain pathological features (like upper motor neuron impairment with spastic reflexes, ataxia, loss of coordinated movement, perivascular infiltration of CD8+ T cells and lesions mostly within the white matter of the cerebellum) observed in MS patients, but which are typically absent in myelin-specific CD4+ T cell-mediated EAE [53].

The CNS has long been referred to as an “immune privileged site” that immune cells cannot access [54], a notion that was reinforced by the anatomical hurdle, the blood-brain barrier (BBB) [55]. However, increasing evidence contradicts this paradigm [56] as CNS antigen was detected to drain to the cervical lymph nodes (LN) [57] and T cells were documented to traffic into the CNS through post-capillary venules [58]. In this context, the individual steps of myelin-specific CD8+ T cell activation to cause CNS inflammation and demyelination in-vivo are thought to be the following

(in a schematic presentation): in the periphery, myelin-specific CD8+ T cells are activated by cross-presenting dendritic cells (for explanation see legend of Fig. 2). After CNS invasion they become re-activated by APCs presenting self-antigen to eventually destroy target cells through release of their effector molecules (see above).

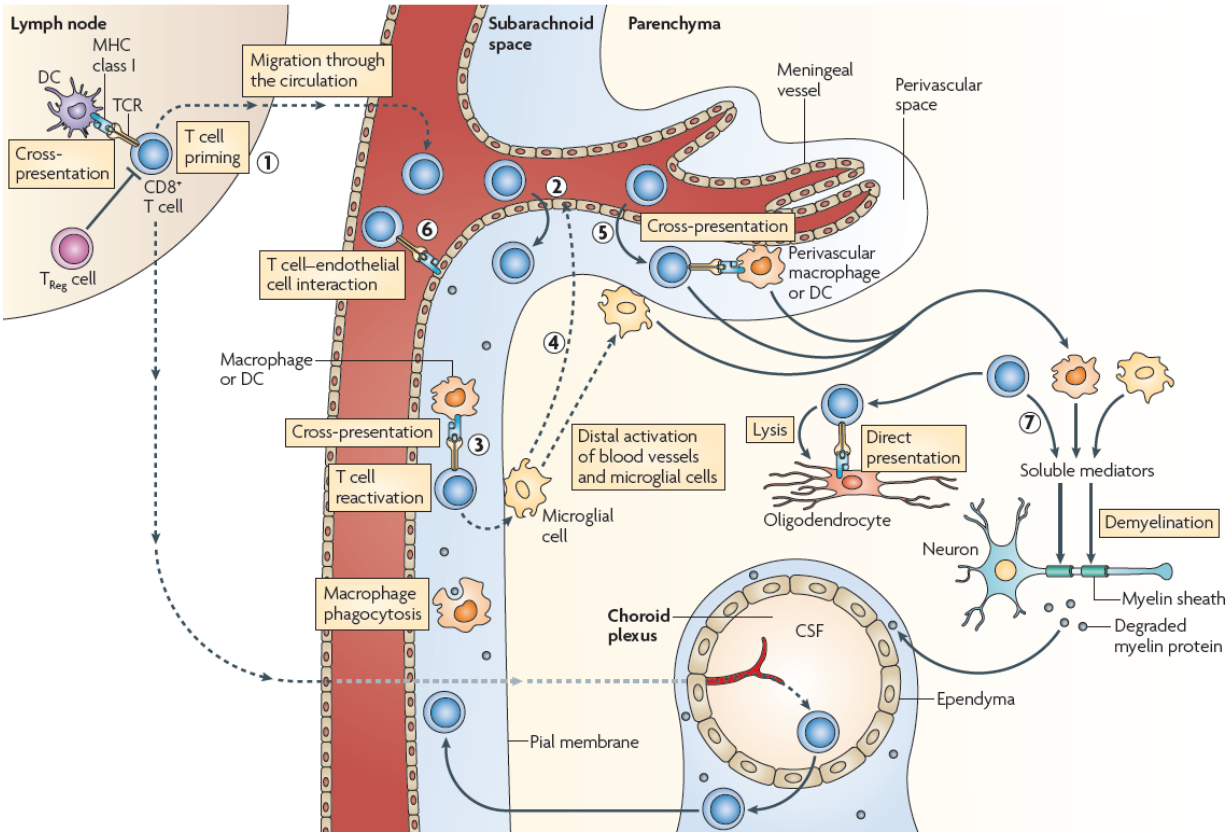

Fig. 2 **Schematic view of myelin-specific CD8+ T cells activation causing CNS demyelination**. In the lymph node, myelin-specific CD8+ T cells become primed by dendritic cells that phagocytosed and processed cell-associated antigens like myelin proteins to present them through the MHC class I pathway (referred to as cross-presentation) (1). Primed CD8+ T cells migrate to the subarachnoid space by crossing the blood brain barrier (2). In the subarachnoid space, T cells are re-activated by macrophages (3), microglia (4) or dendritic cells (5) by cross-presentation or they can be directly activated by endothelial cells (6) if these have access to myelin e pitopes. CD8+ T cells can then kill target cells by either contact mediated

lysis via Fas ligand or by the secretion of soluble mediators like perforin or granzyme eventually causing demyelination and axonal loss (**7**) (adapted to [59]).

1.5 The importance of myelination

As highlighted in the clinical signs of MS (see above) or other diseases with compromised myelin, such as leukodystrophies in the CNS or peripheral neuropathies in the PNS [60], the vertebrate nervous system becomes largely non-functional without a proper myelin sheath. The importance of myelination becomes further emphasized by its evolutionary conservation. All vertebrate classes engulf their axons by myelin membrane wraps of either OLG in the CNS [61] or Schwann cells in the PNS except for jawless fish, in which axons are surrounded likewise to most invertebrates by other glial cell [62].

1.5.1 Structure, function and clinical relevance of myelin

Myelin is a multi-lamellar sheath of OLG plasma membrane wraps in the CNS that holds two major functions: (1) it permits fast, saltatory conduction of the electrical impulse along an axon, (2) it appears to be required for axonal trophic support [63]. To fulfill these functions, myelin has a characteristic ultrastructural morphology and biochemical composition. In the CNS, it engulfs axons that are larger than 0.2 μm in diameter [64] at the internodes that have an average length of 150-200 μm [65]. These are separated by spaces lacking myelin, the nodes of Ranvier, which are about 1 μm in length [66]. The nodes of Ranvier show clusters of voltage-dependent Na^+ channels flanked by fast K^+ channels in the juxtaparanodal region [67]. This myelin morphology together with its insulating lipid content (myelin contains 70% lipids especially cholesterol and glycosphingolipids, 30% proteins and only little water [68]) ensures fast saltatory impulse conduction.

Transmission electron microscopy (TEM) studies observed a characteristic lamellar (rather than concentric) spiral structure of the myelin sheath with an alternation of light and dark layers [69]. These layers turned out to refer to either the intraperiod line (light layer in TEM, in average 150 pm thick), in between which the former extracellular space was present, or to the major dense line (dark layer in TEM, in average 170 pm thick), the former OLG cytoplasm [70]. In addition, in the myelin sheath areas can be observed that still contain cytoplasm. Based on these findings, myelin is divided into compact (no cytoplasm containing) and non-compact (cytoplasm containing) myelin that appears not only at different sites but also contains different sets of myelin proteins. Non-compact myelin is found at the inner, outer or lateral edges of the OLG membranes, the so called inner or outer loop or respectively the paranodal loops at the node of Ranvier (Fig. 3).

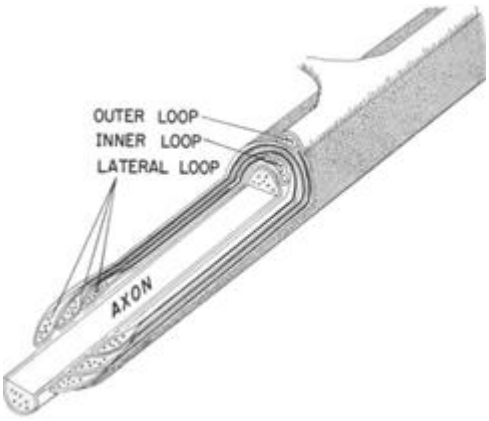

Fig. 3 **Myelin nomenclature**. As depicted, cytoplasm containing non-compact myelin is found at ad- and ab-axonal sites, referred to as inner and outer loop respectively and at the lateral edges of myelin at the unmyelinated nodes of Ranvier, the lateral loops (adapted to [71]).

An extended view on myelin in terms of its biochemical composition, myelin compaction and axonal integrity was obtained from rather rare non-inflammatory, genetic alterations in myelin proteins or lipids.

For example, mice expressing a mutant myelin basic protein (MBP; the MBP isoforms account for ~ 30% of the myelin proteins) with the *shiverer* (*shi*) mutation suffer from generalized intention tremors, convulsion and die a premature death within 50-100 days after birth. Ultrastructural analysis revealed CNS dysmyelination in these mice with tightly compacted myelin at the intraperiod lines but no major dense lines [72]. MBPs suspected role in compaction was confirmed when *shi/shi* mice were rescued after being crossed with transgenic MBP expressing mice [73].

Furthermore, mice carrying the X-chromosomal *jimpy* (*jp*) mutation in proteolipid protein (PLP; PLP is the major myelin protein in the CNS, accounting with its splice variant DM-20 for ~50% of the myelin proteins [74]) show axial body tremors, tonic seizures and also die a premature death [75]. Here, TEM analyses revealed intact major dense lines but severe alterations of the intraperiod line [76]. Accordingly, PLP was suggested to function as a molecular "zipper" by linking apposing membranes to form compact CNS myelin [77]. In addition, PLP appears to be essential for the enrichment of cholesterol, the major lipid of myelin [78]. Mutations in the PLP gene also account for rare human diseases, such as the recessive, X-linked Pelziaeus-Merzbacher disease (PMD) [79], where male patients show ataxia and myoclonic seizures and die shortly after birth.

Besides of the functions of some of these classical myelin proteins, others were only recently identified. For example, in a microarray analysis of healthy versus demyelinated mouse brain the OLG-specific actin binding protein Ermin was found**.** As a non-compact myelin protein it was suggested to cross-link membrane proteins with the OLG cytoskeleton and to interact with Rho GTPases to regulate the OLG cytoskeleton [80]. In addition, CNS myelin contains distinctive radial components [81], built by the tight junction proteins claudin/OSP [82-84]. Recently, one of the few

known axonal-glial interaction partners were identified, formed by a complex of Caspr/paranodin and contactin on the axonal side with neurofascin 155 on the glial membrane [85-87].

1.6 The current concept how myelination is achieved

Despite a fairly detailed knowledge why myelin's proper wrapping and composition is important, only little is known about the wrapping mechanism per se. In light of the fact that at least in the CNS the OLG cell body cannot move to form multilamellar myelin, the assembly of the membranes could formally be achieved by: (1) an active process of the myelinating cell, where the axon remains comparatively passive, (2) an active myelin membrane pulling by the axon, where the myelinating cell remains comparatively passive or (3) a mixture of both.

Surprisingly, the present myelination theories favor the first possibility and neglect the others. The currently most accepted sequence of events for myelination is [88]: (1) an OLG process curls a membrane sheath around an axon, (2) after this sheath completed its first turn, the growing membrane advances itself *under* the already existing membrane wrap as it was crawling underneath a carpet. (3) This procedure of spiral wrapping continues until the final myelin thickness is achieved. (4) The process is accomplished by an unknown mechanism leading to the extrusion of cytoplasm to allow the close apposition of membranes to form compact myelin. (5) The final myelin product would resemble a rolled up carpet with a smooth surface resulting in a parallel run of inner and outer loop (hereafter referred to as "carpet crawler" model; Fig. 4). However, not even a single study up to this date provided satisfying evidence for any of these events. It is thus not surprising that this too simplified model has repeatedly been questioned by other studies (see below).

Historically, Geren *et al*. suggested in their earliest TEM study that myelin develops by an infolding process of the Schwann cell surface based on their observations of chick embryo sciatic nerve [89]. A little later, Luse *et al*. proposed for the CNS that the myelin sheath forms by the joining of membranes from different glial processes as a patchwork quilt of plasma membranes [90]. Others in turn assumed that myelin derives from membranous segments synthesized in the glial cytoplasm, which eventually fuse to from the myelin sheath [91]. In the style of the mechanism for peripheral myelinogenesis, Peters *et al.* suggested an advancement of the glial inner process in the fashion of spiral wrapping, where compact myelin arises by the loss of cytoplasm [92], which was supported by others [93]. Later, this theory, to which we will refer to as the "carpet crawler" theory, was claimed to be proven by an in-vitro live imaging study of myelination. The observation that the Schwann cell nucleus moved around the co-cultured axon during myelination let the authors conclude that this nuclear rotation reflected the movement of the inner glial process to form myelin [88]. However, this "proof" cannot explain CNS myelination, since the OLG cell body has to remain stable when myelinating up to 50 or more different axons.

1.7 The current myelination concept in question

Although each of the studies is rather incomplete as all used either fixed tissue for TEM analysis at a single level or in-vitro co-culture models, the latter hypothesis prevailed, even despite questioning consecutive studies (see below) that used more sophisticated approaches.

For example, Webster *et al.* performed a three dimensional TEM reconstruction from serial sections to obtain a more complete picture of the myelin sheath. As a result, he described an uneven growth of the myelin membranes at different levels of the same internode [94]. This uneven growth, reflected in an inhomogeneous contour of myelin caused most likely by a maximum

thickness near the middle of the internode, was also confirmed by others [95,96]. Further TEM studies noted myelin formations with cytoplasmic inclusions, which could not easily be explained by the established concept and thus asked for a more complex explanation [71]. Later, light microscopic studies showed the spiraling of the ostensibly outer tongue or respectively, the distribution of caspr in a helical coil along the internode [80,82,84,97-99]. That the findings are artifacts or that they are confined to only developing myelin is rather unlikely, as a continuous myelin sheath turnover in the adult CNS was suggested [100]. Since the "carpet crawler" hypothesis, where the myelin outer tongue runs in parallel with the long axis of the axon, cannot explain such features, an alternative myelination model was suggested. There, a myelin ribbon coils unidirectional around the axon like a serpent around a tree, followed by a lateral outgrowth of the ribbon (hereafter referred to as "serpent" model; Fig. 4) [98]. By this lateral myelin outgrowth, the outer loop runs in a coil along the internode resembling a bandage wrapped up for a cast.

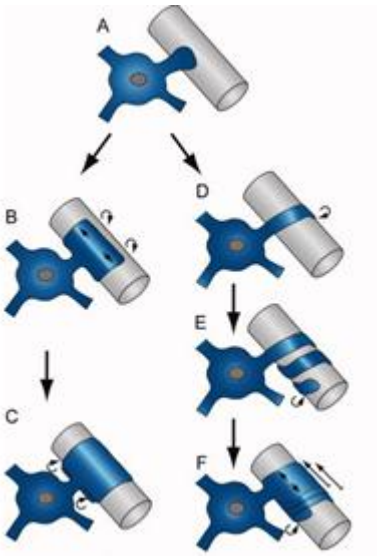

Fig. 4 **Current views on myelin wrapping**. An OLG process comes in close contact with an axon (A). According to the "carpet crawler" hypothesis (B and C) the growing membrane advances itself *under* the already existing membrane wrap until the final myelin thickness is

achieved. In contrast, the “serpent” model (D, E, F) suggests an unidirectional coiling of a myelin ribbon around the axon (adapted to [101]).

It is peculiar that both models assume myelination to be an active process of the myelinating cell, where the axon remains comparatively passive, especially as increasing evidence underlines an axonal contribution Besides, high energy expenditure due to friction caused by the advancement of the inner myelin tongue with constant adhesion and loosening questions the “carpet crawler” model. Likewise, the “serpent” model neither explains the feature of paranodal loops, where the most outer myelin layer is the closest to the node of Ranvier, nor maximum thickness of myelin at the middle of the internode.

2 Rationale

As described above, CD8+ T cells are increasingly believed to participate in the pathophysiology of MS [41,43] but the underlying mechanisms have remained unclear. Particularly, in the past neither of the studies addressed the pathogenic role of myelin-reactive CD8+ T cells with regard to axonal damage. To clarify whether myelin-reactive, cytotoxic CD8+ T cells directly attack axons or whether axonal loss may be the result of a targeted hit against myelinated structures indicating "collateral bystander damage", we established a novel experimental system of inflammatory CNS injury:

Auto-aggressive, cytotoxic ovalbumin (OVA)-TCR CD8+ T cells (OT-I T cells) were traced in real time by continuous confocal imaging in living PLP-GFP (see later) derived cerebellar brain slices [102]. In an inflammatory environment, we either loaded brain tissue with the cognate OT-I T cell antigen, the peptide SIINFEKL, or we restricted OVA expression exclusively to the cytosol of OLG by crossing PLP-GFP mice with transgenic mice where OVA is sequestered to OLG (ODC-OVA mouse [103]). Live imaging and subsequent morphological analysis let us demonstrate that axonal loss can be the consequence of "collateral bystander damage", resulting from a CD8-mediated attack directed against the cognate antigen processed and presented by OLG.

On the basis of the controversy on myelin formation presented above, the cellular mechanisms of CNS myelination remain an interesting and challenging problem. To clarify myelin formation in the CNS, we performed a comprehensive high-resolution live imaging, light and electron microscopy study in organotypic cerebellar slice cultures (OCS), young and adult CNS derived from transgenic PLP-GFP mice, which carry a fusion-protein of the first 13 transmembrane amino acids of proteolipid protein (PLP) with green fluorescent protein (GFP) [102] (and B. Zalc,

personal communication). Our results show clearly an evenly spaced, bi-directional coiling of the myelin outer loop that developed during myelin formation and that was present in both young and adult mice. Based on our observations and supporting evidence discussed below, we proposed a new myelination hypothesis, the “liquid croissant” model”. Our concept resolves not only the current, most suspected concerns and explains previous observation but it attributes a yet unaddressed function to the axon, which may help to explain myelination deficits during remyelination or axonopathies.

3 Materials and Methods

Mice. Mice (all C57BL/6 background) were bred at the animal facilities of the University of Zurich under specific pathogen-free conditions, and all experimental procedures were approved by the Swiss Veterinary Office (121/2009). OT-I and OT-II mice carrying a transgenic T cell receptor (TCR) specific for ovalbumin (OVA) amino acids 257-264 (SIINFEKL) in H-2K^b or for $OVA_{323-339}$ in H-2IA^b, respectively, were obtained from The Jackson Laboratory (USA). 2D2 transgenic mice carrying CD4+ T cells with a TCR reactive for MOG_{35-55} were kindly provided by V. Kuchroo (Boston, USA) and ODC-OVA (oligodendrocyte-ovalbumin) transgenic mice were obtained from T. Hünig (Würzburg, Germany) and were genotyped as defined elsewhere [103]. PLP-GFP transgenic mice were a kind gift from B. Zalc (Paris, France). The original PLP-LacZ mouse [104] was described to show a similar expression pattern of the PLP-LacZ fusion protein when compared to endogenous PLP. It was modified subsequently [102] by replacing LacZ with EGFP to generate the PLP-GFP mouse (B. Zalc personal communication) which carries a PLP-EGFP fusion protein.

Genotyping. A small biopsy of mouse tail dissolved in tail lysis buffer (100 mM Tris/HCl pH 7.5, 1M Tris pH 7.5, 5 mM EDTA, 0.5M EDTA, 0.2% (w/v) SDS, 200 mM NaCl, 10mg/ml proteinase K) at 55 °C for 4 h. After precipitation in isopropanol and washing with 70 % ethanol samples were diluted in TE buffer and stored at -20 °C. Genotyping of PLP-GFP mice was performed using the following primers: for PLP-GFP forward 5'-CAA AAC AGC TGT CTG TAT ATC ATG CTT GC-3'; PLP-GFP reverse 5'-GTG GAT GAG TTA CCT CGT ATG CGT ACC-3' with an annealing temperature at 57 °C; primers for the other mice described above are defined in the respective references.

Organotypic cerebellar slice culture. To study (patho)physiological processes in the CNS, we obtained organotypic cerebellar slice cultures (OCS) from 8 to 10-day-old mice, in which the brain parenchyma is preserved in a proper network organization ex-vivo [105]. After decapitation the cerebellum was removed and put into ice-cold dissecting medium (HBSS (Invitrogen, Basel, Switzerland) supplemented with penicillin/streptomycin (Invitrogen; 100 U/ml and 100 μg/ml respectively), 2.5 mg/ml glucose and 10 mM kynurenic acid (both by Sigma, Buchs, Switzerland). It was then cut with a McIllwain tissue chopper (GaLa Instruments, Bad Schwalbach, Germany) into 400-500 μm thick cerebellar slices. OCS were cultured on Millicell plate inserts, pore size 0.4 mm (Millipore, Zug, Switzerland) according to Stoppini *et al.* [106] in culture medium (50 % (v/v) MEM, 25 % (v/v) HBSS, 25 % (v/v) heat-inactivated horse serum, supplemented with penicillin/streptomycin (100 U/ml and 100 μg/ml respectively), 2 mM L-glutamine (all from Invitrogen) and 2.5 mg/ml glucose (Sigma). OSC were incubated at 36 °C in a humidified atmosphere with 5% CO_2 for at least 7 days to allow tissue flattening [105]. Where indicated, slice culture medium was supplemented with 100 U/ml IFNγ (Preprotech, USA) 72 h prior to co-culture experiments.

Activation and enrichment of T cells. Splenocytes were obtained from euthanized OT-I, OT-II and 2D2 mice and were cultured in RPMI supplemented with 10 % (v/v) heat-inactivated foetal calf serum, penicillin/streptomycin (100 U/ml and 100 μg/ml respectively) and 5 mM L-glutamine (all by Invitrogen). OT-I cells were stimulated with their cognate antigen SIINFEKL peptide or $Smcy_{738-746}$ (H-Y) control peptide (5 μg/ml, GenScript Corp., USA). OT-II and 2D2 splenocytes were incubated with their cognate antigen $Ovalbumin_{323-339}$ peptide or MOG_{35-55} peptide (both 5 μg/ml, GenScript Corp.), respectively. Splenocytes were kept for 24 h in culture medium only for non-activation or were incubated with anti-CD3 antibody (5 μg/ml, Bioexpress,

USA) for unspecific stimulation. Supernatants were analysed for IFNγ production and T cells were enriched by negative selection according to the manufacturer's instructions (Mouse CD8 or respectively CD4 T Lymphocyte Enrichment Set by BD Biosciences, USA). Enriched T cell populations were labelled with the infrared DiD lipophilic tracer (Invitrogen) according to manufacturer's instructions. 24 h prior to time lapse imaging, T cells were applied on cerebellar slices ($1x10^6$ cells/slice), placed on ibiTreat chambers (ibidi, Germany) to allow T cell tissue invasion.

CNS tissue preparation for cryostat sections. Mice were perfused with 4 % (w/v) freshly prepared paraformaldehyde (PFA; Sigma) in 0.1 M phosphate buffer, pH 7.4 at room temperature (RT) with 200 ml/mouse within 15 min and CNS tissue was post-fixed for 48 h in 4% PFA after removal. Tissue was then equilibrated with 30 % sucrose and was frozen with Tissue-Tek (Qiagen, Hombrechtikon, Switzerland) in isopropanol cooled to – 40 °C. Tissue was cut with a cryostat into 40 μm thick for free floating sections.

Confocal time lapse imaging. For confocal live imaging, slices were placed on ibiTreat chambers (ibidi, Munich, Germany). Myelin and T cells in slices were visualized by an SP5 Leica motorized confocal laser scanning microscope (SP5; Leica, Heerbrugg, Switzerland) using an Argon laser with a 20 x objective (oil immersion, numerical aperture (NA) 0.7, Leica) or a 63 x objective (glycerol immersion, numerical aperture (NA) 1.3, Leica) as indicated. Slices were maintained in an incubation chamber at 36 °C using a heated stage and 36 °C warm slice culture medium was equilibrated with 95% O_2 and 5% CO_2. Three dimensional datasets were acquired every 5-45 min over periods as indicated.

Immunostaining. OCS were fixated in 4 % (w/v) formaldehyde for 2 h at RT and were permeabilized in 1 % (v/v) Triton X-100 (both in PBS; both by Sigma). After three washes in PBS, OCS were blocked for 1 h at RT with 10 % (v/v) normal goat serum (Invitrogen) in 0.2 % (v/v) Triton X-100 in PBS. Primary antibodies were diluted in 1 % (v/v) goat serum in 0.2 % (v/v) Triton X-100 in PBS and were incubated with OCS for 3 days at 4 °C. After three washes in PBS, secondary antibodies diluted in 1% (v/v) goat serum in 0.2 % (v/v) Triton X-100 in PBS were added overnight at 4 °C. After three washes in PBS, OCS were mounted on glass slides.

Antibodies. For primary antibodies monoclonal mouse anti-murine neurofilament 200 antibody (clone N52; Sigma-Aldrich, Buchs, Switzerland), monoclonal mouse anti-murine MOG (ms8-18c5 hybridoma, kindly provided by C. Linnigton, Glasgow, UK), monoclonal rat anti-murine MBP (Serotec, Dusseldorf, Germany), polyclonal rabbit anti-murine PLP (Abcam, Cambridge, UK), polyclonal rabbit anti-murine paranodin (kindly provided by J.-A. Girault, Paris, France), monoclonal rat anti-murine MHC class I (clone ER-HR52, BMA Biomedicals, Switzerland) or monoclonal rat anti-murine MHC class II (clone M5/114.15.2, BD, UK) were used as indicated and were detected with secondary goat anti-mouse Alexa Fluor 405-conjugated antibody, goat anti-rabbit Alexa Fluor 546-conjugated antibody or goat anti-rat Alexa Fluor 594 or 633-conjugated antibody (all by Invitrogen).

Laser scanning confocal microscopy, image analysis and video processing. Confocal microscopy from fixed and immunostained slices was performed using an SP2 or SP5 confocal laser microscopes (Leica) with 10 x (dry, NA 0.5), 20 x (glycerol immersion, NA 0.7) or 63 x (glycerol immersion, NA 1.3) objectives. Image series from fixed and stained slices and sequences from time lapse imaging including *z*-stacks were collected in an optimized manner (z steps 0.13 μm) to allow subsequent deconvolution using Huygens deconvolution software SVI

(distributed by Image Solutions, Preston, UK). Images were analysed using Imaris software (version 7.1, Bitplane, Zurich, Switzerland) and videos were processed using Adobe After Effect (version CS4; Adobe, San Jose, USA) or FinalCutPro (version 6.01, Apple, USA).

High pressure freezing, transmission and scanning electron microscopy (TEM and SEM). OCS were high-pressure frozen using a Leica EM HPM100 high-pressure freezing machine (Leica Microsystems, Vienna, Austria). For that, the whole cerebellar slice including culture membrane was excised with a 4 mm biopsy punch (Kai Medical Nr. BPP-40F, Poymed Medical Center, Glattbrugg, Switzerland) on a Teflon surface and was transferred into a 6 mm aluminium specimen carrier with an indentation of 5 mm x 0.1 mm. Excessive medium was drawn off with a filter paper and the head space was filled with 1-hexadecene (Sigma-Aldrich). The sandwich was completed with a flat 6 mm aluminium specimen carrier and moved to the recess in the middle plate of the cartridge to be immediately high-pressure frozen. Frozen specimens were freeze-substituted in anhydrous acetone containing 2 % OsO_4 in a Leica EM AFS2 freeze-substitution unit (Leica Microsystems). Specimens were kept successively at -90 °C, -60 °C, and at -30 °C for 8 h each. Temperatures were changed at a rate of 30 °C per hour, finally reaching 0 °C. After keeping the specimens at 0 °C for 1 h, OsO_4 was removed by washing the specimens with anhydrous acetone twice. For transmission electron microscopy, specimens were gradually embedded in Epon/Araldite (Sigma-Aldrich) 33% in anhydrous acetone overnight at 4°C, 66% in anhydrous acetone for 6 h at 4°C and 100% for 1h at room temperature prior to polymerization at 60°C for 48 h. Ultrathin sections were stained with aqueous uranyl acetate 2 % and Reynolds lead citrate and imaged with a Phillips CM 100 transmission electron microscope (FEI, Eindhoven, Netherlands) using a Gatan Orius CCD camera and digital micrograph acquisition software (Gatan GmbH, Munich, Germany). For scanning electron microscopy, specimens were

critically point dried in a CPD 030 (Leica Microsystems). Tissue pieces were removed from the filter, fractured and mounted on SEM stubs with conductive carbon with the fractured cross-section facing upwards. Samples were sputtered with 4 nm of platinum or gold/palladium in a SCD 500 sputter coater (Leica Microsystems) and imaged in a Zeiss Supra 50 VP scanning electron microscope (Gloor Instruments, Uster, Switzerland) at 10 kV using the in lens secondary electron detector.

3D myelin modelling. 3D myelin was modelled using Strata 3D software (version 5.5.1, Macromedia, Santa Clara, USA).

Statistical analysis. Data were obtained from at least three independent experiments performed in duplicate or triplicate. Results were expressed as means ± standard error of the mean (S.E.M.). Statistical significance of mean differences was assessed by one-way ANOVA followed by Bonferroni post-test using GraphPad Prism software (version 4.02, San Diego, USA).

4 Results

4.1 Axonal loss by myelin-directed CD8+ T cells

In order to investigate if auto-aggressive, cytotoxic CD8+ T cells can potentially cause axonal loss by "collateral bystander damage", we established confocal live imaging in a model system of CNS inflammation.

4.1.1 IFNγ up-regulates MHC class I expression on myelin

To obtain an inflammatory environment, living brain slices were pre-incubated with the pro-inflammatory cytokine IFNγ, described to enhance MHC expression. Subsequent confocal microscopic analysis of fixed slices, stained for neurofilament (NF) and either MHC class I or MHC class II molecules, demonstrated that both MHC class molecules were differentially inducible upon treatment with IFNγ (Fig. 5). As expected, MHC class II was neither observed on myelin nor axons but on microglia (Fig. 5B), whereas MHC class I expression was most pronouncedly identified on myelin (Fig. 5C and subset of C). As such, IFNγ-induced up-regulation of MHC class I molecules ensured the key prerequisite for antigen presentation to and recognition by CD8+ T cells [107].

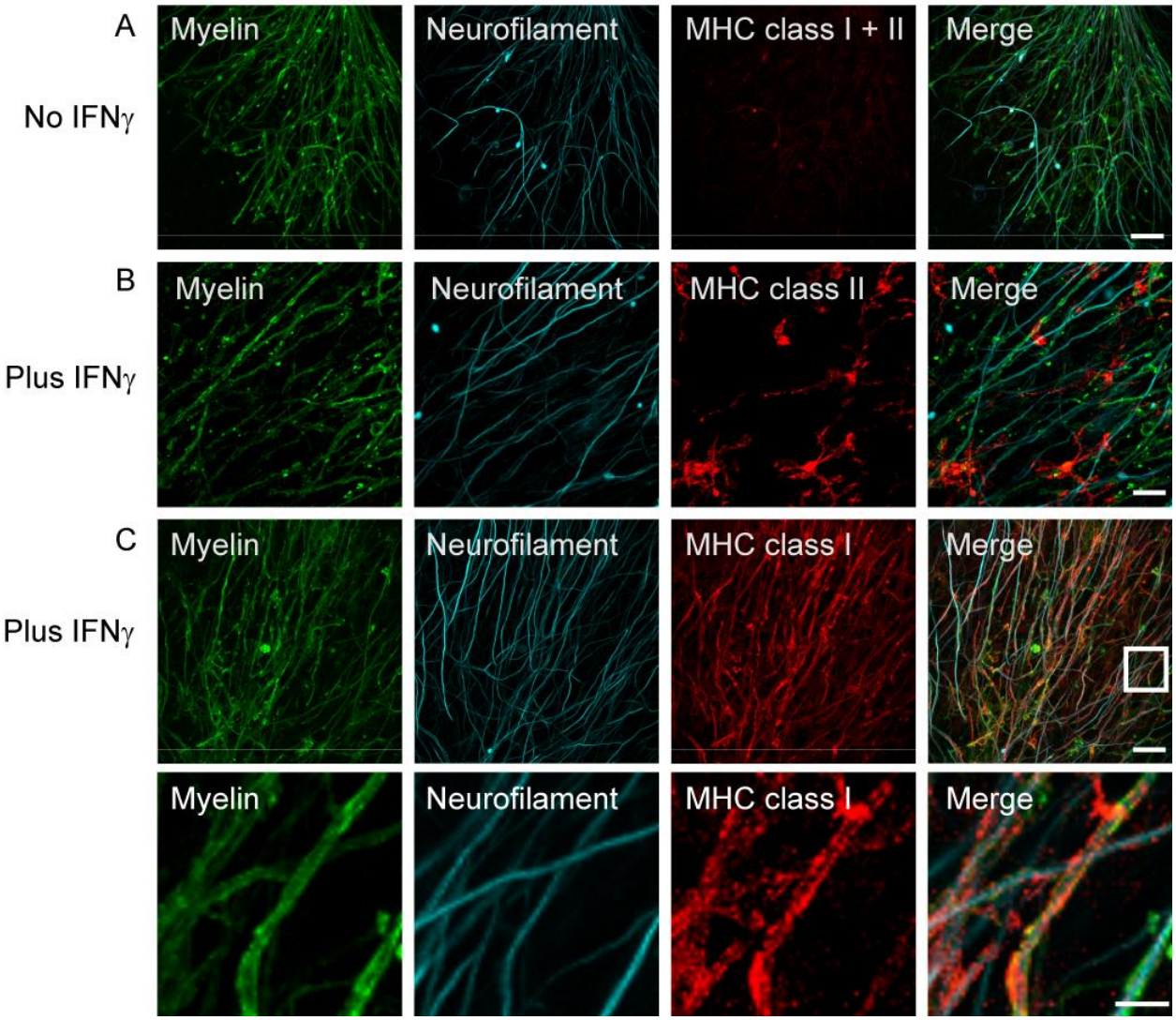

Fig. 5 **Incubation with IFNγ induces MHC class I and II expression**. Confocal images of co-stained MHC class I and II (red) and NF (cyan) reveal only marginal MHC expression in untreated ODC-OVA x PLP-GFP brain slices (A). Yet, presence of IFNγ (100 U/ml, 72h) induces MHC expression (B, C). Whereas MHC class II was most likely observed on microglia (B), MHC class I was mainly induced on OLG (C and lower panel of C). Scale bars equal 20 μm in (A, B and C) and 7.5 μm for lower panel in (C).

4.1.2 CD8 + T cells cause myelin damage in SIINFEKL pulsed OCS

To assess the impact of cytotoxic CD8+ T cells on axonal injury, we pulsed IFNγ pre-treated brain slices from PLP-GFP mice with ovalbumin (OVA) peptide$_{257-264}$ (SIINFEKL). Addition of SIINFEKL pre-stimulated CD8+ OT-I T cells (Fig. 6 B, D) resulted in direct injury of myelinated fibers (Fig. 7B). In contrast, application of CD4+ OT-II T cells onto PLP-GFP brain slices loaded with MHC class II OVA peptide$_{323-339}$ (Fig. 6A, C) left myelin and axons intact in the previously described experimental set-up (Fig. 7A).

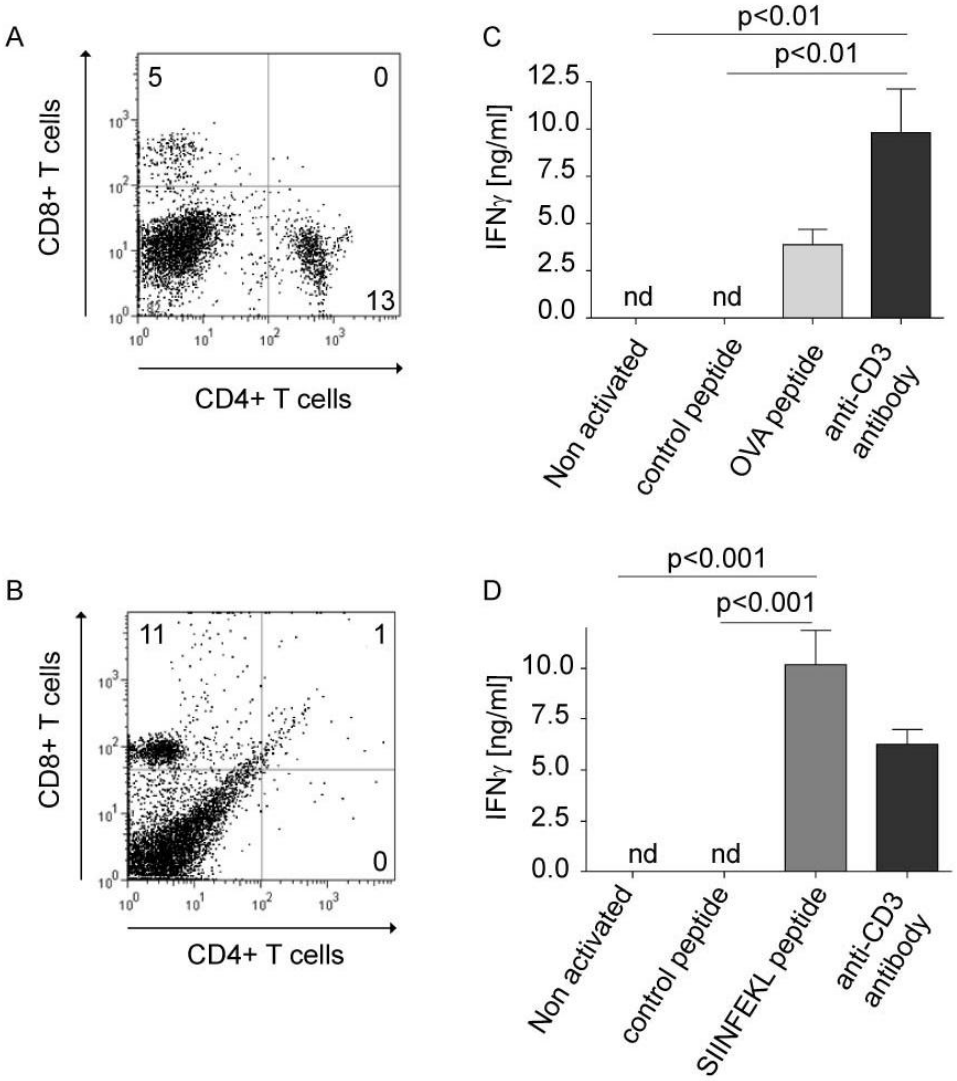

Fig. 6 **Antigen-specific stimulation results in specific activation of T cells**. Flow cytometric stains show the ratio of CD4+ compared to CD8+ T cells in OT-II (A) and OT-I (B) whole splenocytes. Whole splenocytes from either OT-II (C) or OT-I (D) mice were stimulated for 24 h as indicated and supernatants were subjected to quantitative IFNγ ELISA (C, D) displaying significantly increased IFNg secretion of CD8+ OT-I T cells when incubated with cognate peptide (SIINFEKL). Note, that OT-I splenocytes contain mostly CD8+ T cells (B), while OT-II splenocytes contain both CD4+ and CD8+ T cells (A), which may account for the differences in IFNg secretion when stimulated with cognate peptide vs. anti-CD3 antibody (C, D). Nd= non-detectable; values are ± mean S.E.M., n=3, for p-value generation one-way ANOVA followed by Bonferroni post test was used to compare among groups.

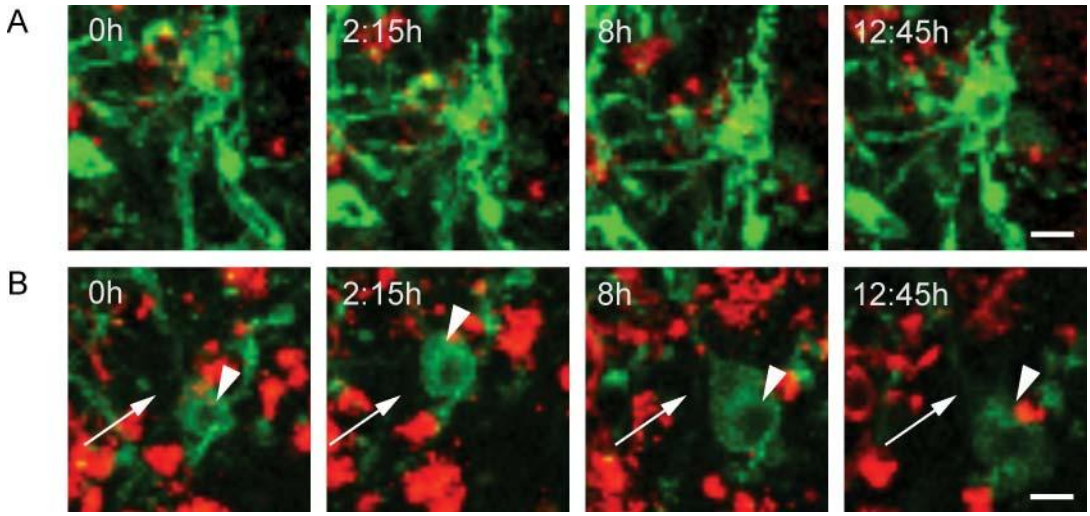

Fig. 7 **SIINFEKL pre-stimulated CD8+ OT-I T cells cause myelin damage in SIINFEKL pulsed PLP-GFP brain slices**. PLP-GFP brain slices, pre-treated with IFNγ and pulsed with OVA peptide323-339 (A) or SIINFEKL (B) peptide were incubated with OVA peptide323-339 pre-stimulated CD4+ OT-II T cells (A) or SIINFEKL pre-stimulated CD8+ OT-I T cells (B). Whereas no change in myelin morphology is observed when adding OVA peptide323-339 pre-stimulated CD4+ OT-II T cells (A), SIINFEKL pre-stimulated CD8+ OT-I T cells closely interact and damage myelin (B). In the upper left corner time elapsed after start of the respective sequence is documented, scale bars equal 15 μm.

4.1.3 CD8+ T cells cause axonal loss even when the antigen is restricted to OLG

Although we observed CD8-mediated axonal damage in peptide-pulsed brain slices, in which we could not detect MHC class I expression by axons, we could not formally exclude the possibility that the peptides loaded onto the brain slices were presented by axons. To specifically address the question whether axonal loss is the result of a direct T cell-axon recognition or driven primarily by an attack against the myelin sheath, we restricted the cognate T cell antigen expression to OLG. We therefore refined our system by crossing PLP-GFP mice with transgenic mice expressing OVA in the cytosol of OLG only (ODC-OVA x PLP-GFP mice).

SIINFEKL or anti-CD3 antibody (data not shown) pre-stimulated CD8+ OT-I T cells directly attacked and transected myelinated axons in ODC-OVA x PLP-GFP brain slices, causing extensive tissue injury (Fig. 8C, D). Yet, the observed pathology was neither detected when applying (i) non-activated (Fig. 8A), nor (ii) control peptide pre-stimulated CD8+ OT-I T cells (Fig. 8B), nor when adding (iii) adequately pre-stimulated CD8+ OT-I cells to ODC-OVA negative slices (data not shown) or (iv) ODC-OVA positive slices not pre-exposed to IFNγ (data not shown).

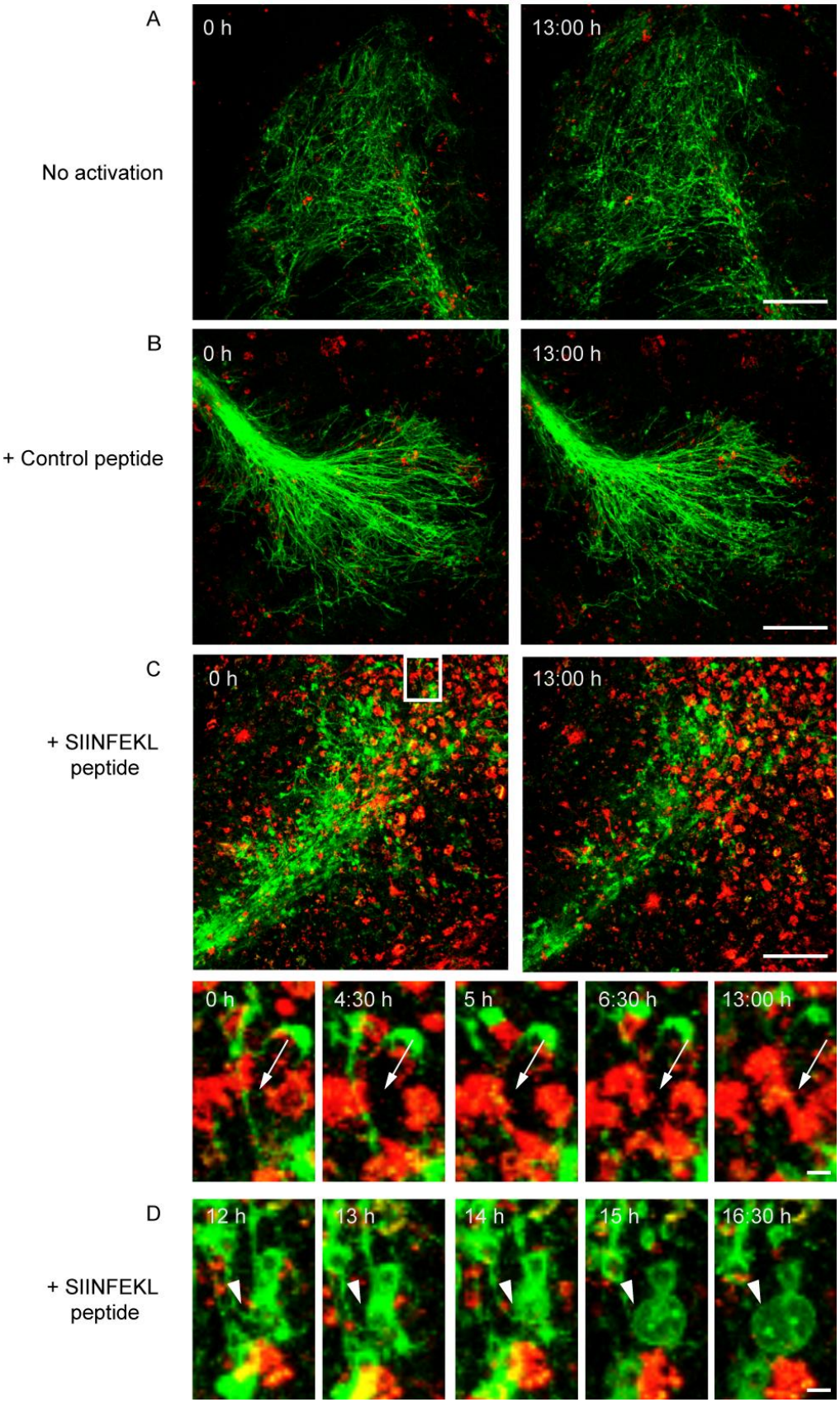
A
No activation
0 h
13:00 h
B
+ Control peptide
0 h
13:00 h
C
+ SIINFEKL peptide
0 h
13:00 h
0 h
4:30 h
5 h
6:30 h
13:00 h
D
+ SIINFEKL peptide
12 h
13 h
14 h
15 h
16:30 h

Fig. 8 **Direct transsection of myelinated axons by CD8+ OT-I T cells**. Frames from confocal time lapse sequences were captured and document only little invasion of non-activated (A) or control peptide (B) pre-stimulated CD8+ OT-I T cells (red) into ODC-OVA x PLP-GFP brain slices. Myelin damage was not observed in either situation (A, B). Contrarily, SIINFEKL pre-stimulated CD8+ OT-I T cells entered brain slices to great extent (C) and directly attacked myelin (green) (subregion of (C)). Additionally, pronounced blebbing of OLG after T cell attack was observed (D). In the upper left corner time elapsed after start of sequence is documented, scale bars equal 30 μm in (A, B and C) and 10 μm for sub-region of (C) and in (D).

Equally, loading of IFNγ pre-treated PLP-GFP brain slices with whole ovalbumin protein did not cause OT-I-mediated CNS injury (Fig. 9).

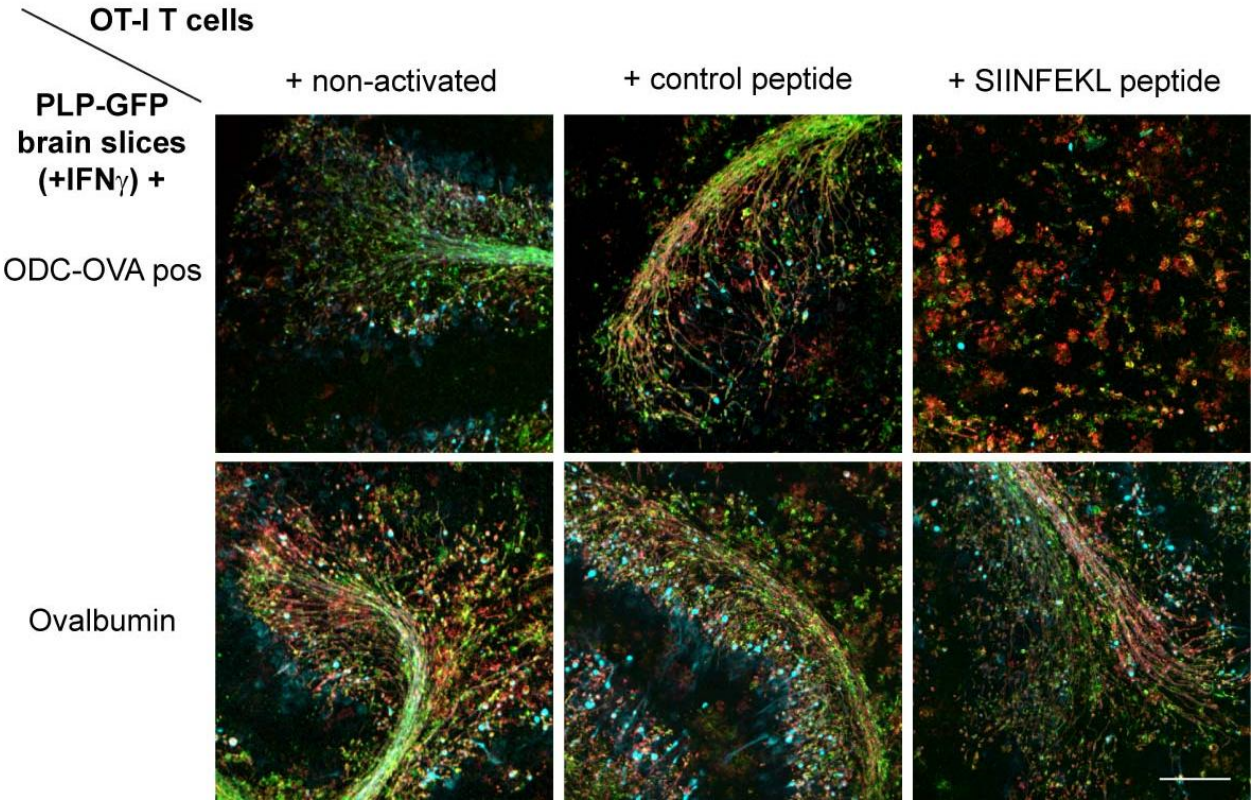

Fig. 9 **SIINFEKL pre-stimulated CD8+ OT-I T cells do not cause myelin damage when pulsing PLP-GFP brain slices with complete ovalbumin protein**. Immunostaining for

neurofilament (cyan) and myelin basic protein (MBP; red) reveals that SIINFEKL pre-stimulated CD8+ OT-I T cells leave myelin and axons intact in PLP-GFP brain slices pulsed with complete ovalbumin protein (lower panel). In contrast, myelin and axons are extensively damaged by SIINFEKL pre-stimulated CD8+ OT-I T cells in ODC-OVA x PLP-GFP brain slices (upper panel). Scale bar represents 150 μm.

In addition, both CD4+ OT-II and 2D2 T cells left myelin and axons intact in IFNγ pre-treated ODC-OVA x PLP-GFP brain slices (Fig. 10).

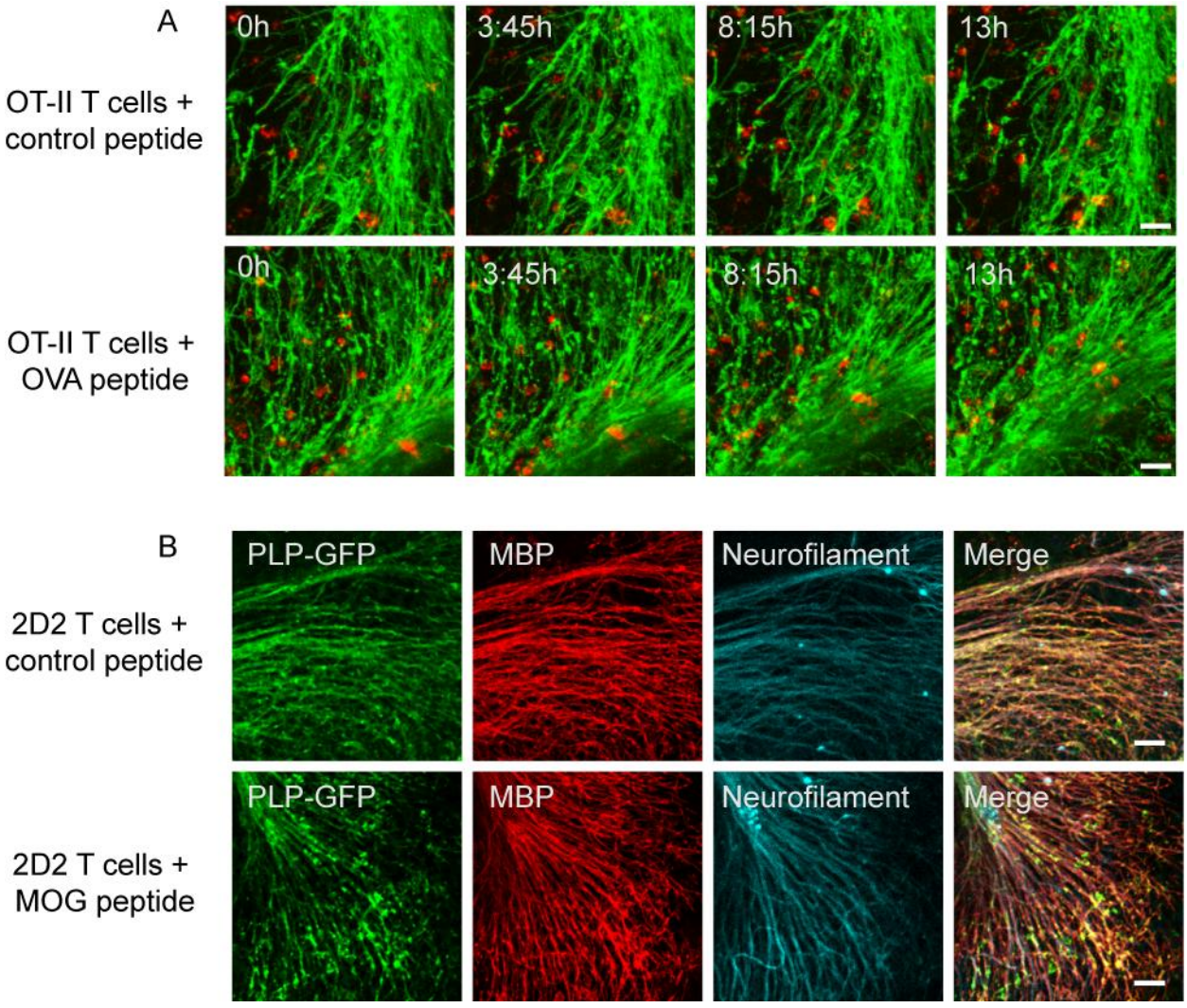

Fig. 10 **CD4+ OT-II and 2D2 T cells leave myelin and axons intact in ODC-OVA x PLP-GFP brain slices**. (A) Frames from confocal-time lapse sequences were captured displaying

myelin in green and differentially pre-stimulated OT-II T cells in red as indicated. No alteration of myelin morphology can be observed in either situation (A-C). (B) Immunostaining for neurofilament (cyan) and myelin basic protein (MBP; red) from fixed ODC-OVA x PLP-GFP brain slices show no alteration in axonal and myelin morphology after incubation with differentially pre-stimulated 2D2 T cells as indicated. In the upper left corner time elapsed after start of the respective sequence is documented, scale bars represent 30 μm in (A) and 50 μm in (B).

Injury of myelinated axons appeared to correlate directly with CD8+ T cell migration into and interaction with the brain parenchyma. Spot analysis from *z*-stacks of confocal time lapse imaging underscored that SIINFEKL peptide pre-stimulated OT-I T cells invaded IFNγ pre-treated ODC-OVA x PLP-GFP brain slices to significantly greater extent than did non-activated or control peptide pre-stimulated OT-I T cells (Fig. 12). Additionally, longer lasting interactions of SIINFEKL pre-stimulated OT-I T cells with CNS tissue were observed when compared to non-activated and control peptide pre-stimulated T cells. In line, trajectory analysis revealed a "scanning" behavior of SIINFEKL pre-stimulated OT-I T cells whereas non-activated or control peptide pre-stimulated T cells displayed a "straight forward" motion (Fig. 11), similarly to that behavior described for CD4+ T cells [108]. As such, CD8-mediated CNS injury appeared to depend both on the T cell activation status and the cognate antigen being presented by MHC class I expressing OLG.

Fig. 11 **Heterogenous migration behavior of CD8+ OT-I T cells**. Analysis of time lapse imaging of CD8+ OT-I T cells on ODC-OVA x PLP-GFP slices shows that CD8+ OT-I T cell migration is variable in direction and distance as depicted in tracings of migratory paths (A, non-activated; B, control peptide pre-stimulated; C, SIINFEKL pre-stimulated). Trajectories, shown for an elapsed time of 16 h, also illustrate mobile and immobile CD8+ OT-I T cell behavior, as well as transition between the two modes.

Subsequent morphological analysis of ODC-OVA x PLP-GFP brain slices exposed to SIINFEKL peptide pre-stimulated OT-I T cells revealed widespread, patchy disintegration of axonal morphology (Fig. 12A and B). Quantification of axonal injury confirmed significantly more axonal loss in ODC-OVA x PLP-GFP brain slices exposed to SIINFEKL peptide pre-stimulated OT-I T cells when compared to controls (Fig. 12D).

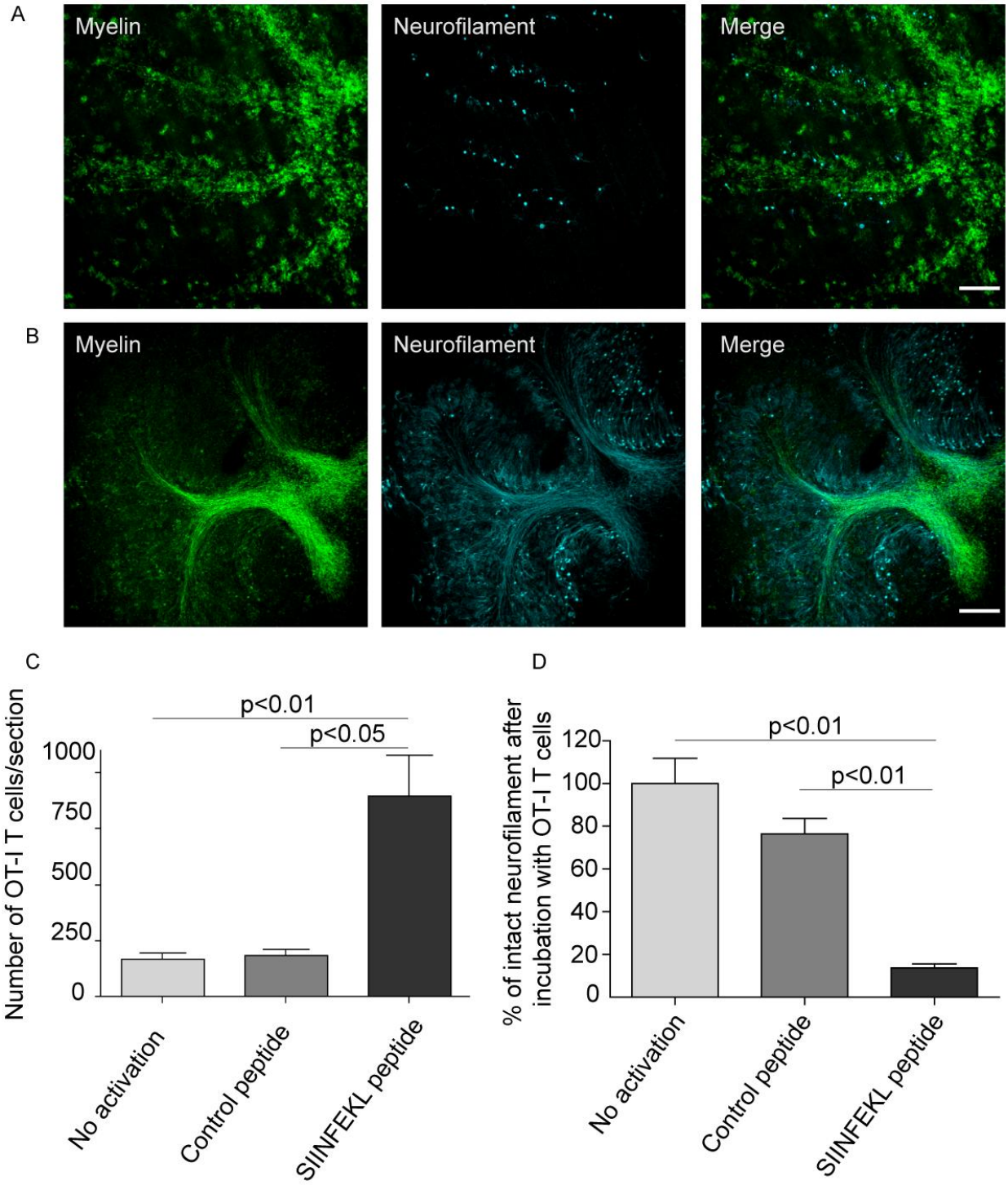

Fig. 12 **SIINFEKL pre-stimulated cytotoxic OT-I T cells invade brain tissue and cause damage of myelinated axons**. Spot analysis from confocal time lapse imaging revealed that SIINFEKL pre-stimulated CD8+ OT-I T cells invaded ODC-OVA x PLP-GFP slices to a significantly greater extent than non-activated or control peptide pre-stimulated CD8+ OT-I T

cells (C). Extensive disruption and irregularities of both myelin (green) and axons (cyan) in ODC-OVA x PLP-GFP brain slices were observed after incubation with SIINFEKL pre-stimulated CD8+ OT-I T cells (A) in contrast to well-maintained structures in slices incubated with non-activated CD8+ OT-I T cells (B). Quantification of axonal damage confirms that neurofilament was significantly injured in ODC-OVA x PLP-GFP brain slices incubated with SIINFEKL pre-stimulated CD8+ OT-I T cells when compared to controls (D). Results are expressed as percentage of intact neurofilament compared to ODC-OVA x PLP-GFP brain slices incubated with non-activated CD8+ OT-I T cells. Values are ± mean S.E.M., n=3, for p-value generation one-way ANOVA followed by Bonferroni posttest was used to compare among groups (C, D). Scale bars equal 200 μm in (A, B).

As expected, the CD8+ T cell release of cytotoxins like perforin appeared to participate in the damage of myelinated axons suggested by the polarized location of perforin towards the myelinated axon (Fig. 13).

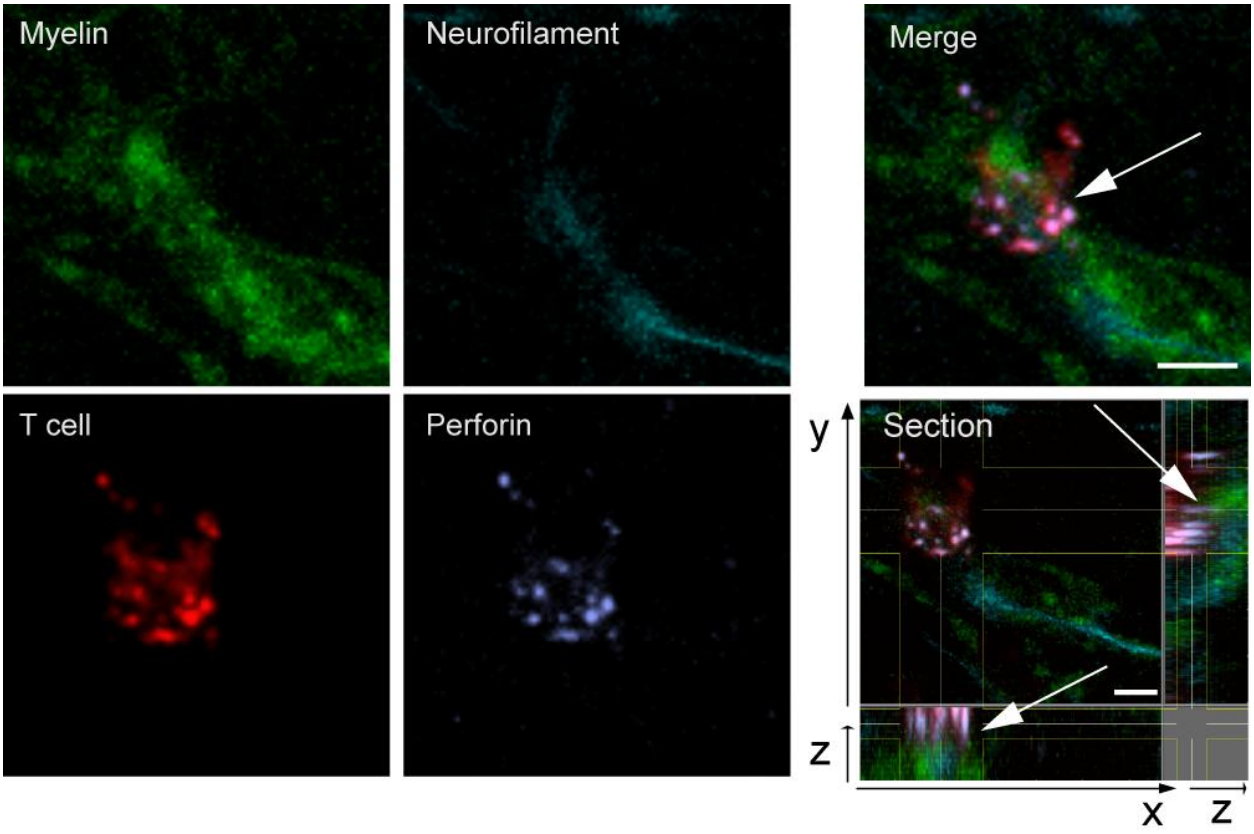

Fig. 13 **OT-I T cells polarized perforin towards myelinated axons**. OCS incubated with OT-I T cells (red) were fixated and stained for Neurofilament (cyan) and perforin (purple). Confocal analysis revealed that perforin granules were polarized towards myelin (green) surrounding an axon (cyan), best observed in the section view displaying the z-plane. Scale bars equal 5 μm.

In conclusion, we could show in our experimental system, in which the cognate antigen was sequestered to oligodendrocytes exclusively, that oligodendrocytes are capable of processing and presenting antigen to auto-aggressive, cytotoxic CD8+ T cells. In turn, CD8+ T cells directly targeting the myelin sheath cause axonal loss due to "collateral bystander damage".

4.2 Myelin formation in the CNS

To examine myelination in the CNS, we performed high-resolution live imaging, light and electron microscopy study in organotypic cerebellar slice cultures (OCS), young and adult mouse CNS. As a model system for myelin live observation, we used OCS derived from transgenic PLP-GFP mice [102]. In these mice, a fusion-protein of the first 13 transmembrane amino acids of proteolipid protein (PLP) with green fluorescent protein (GFP) is expressed under the PLP promoter and has previously been described to show a similar localization to endogenous PLP [104].

4.2.1 Myelin runs in a bi-directional coiled turn along the internode

We first verified the suitability of PLP-GFP mice derived OCS to ensure that the observed PLP-GFP could indeed reflect myelin formation. A comparison of PLP-GFP with endogenous PLP by means of colocalization analysis revealed a similar expression pattern as described previously[104], allowing the visualization of both myelin and mature oligodendrocytes (Fig. 14a, b). We further confirmed intact CNS morphology in OCS by light and electron microscopy which resembled in-vivo CNS tissue, thus validating OCS as a proper model system (Fig. 14c, d).

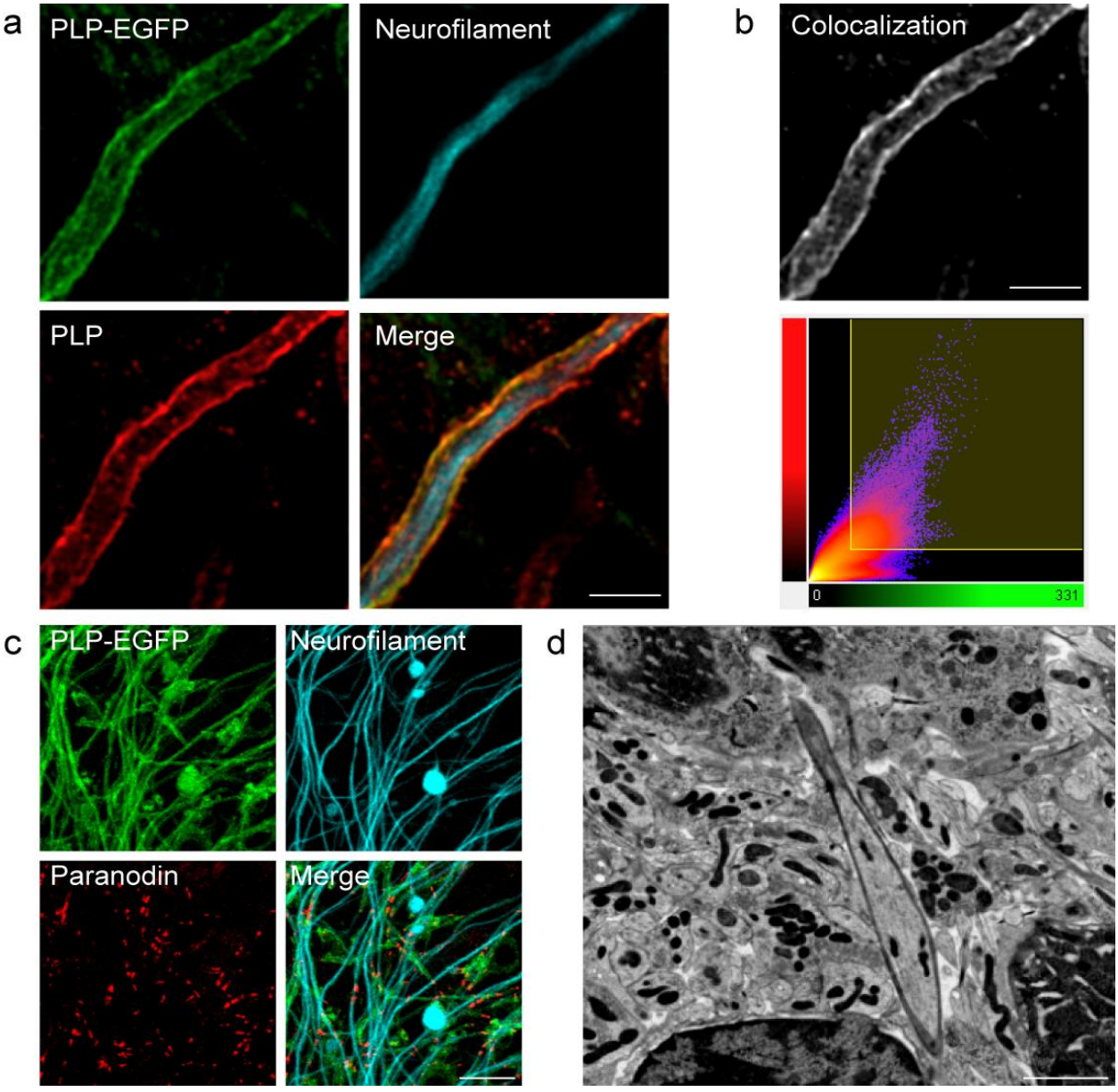

Fig. 14 **Slice cultures derived from PLP-GFP mice appear suited as a model system to study myelination**. (a) Fixed OCS derived from PLP-GFP (green) mice were stained with PLP (red) and NF (cyan). (b) Comparison of endogenous PLP with PLP-GFP show a similar distribution around the axon, confirmed by the white fluorescence representing colocalization. For colocalization analysis serial optical sections were acquired in an optimized manner to calculate Pearson coefficients after deconvolution analysis. Morphologically intact CNS tissue in OCS was found both by (c) paranodin staining (red) implying proper nodes of Ranvier and (d) ultrastructural TEM analysis. Scale bars equal 3 μm in (a, b), 20 μm in (c) and 1 μm in (d).

High-resolution confocal imaging in OCS was superior to multi-photon imaging (data not shown) and displayed coiled turning of myelin (Fig. 15a) that typically, but not exclusively ran bi-directionally along the internode as seen in the slice view (Fig. 15b) resembling the bi-directionally spiralling dough edges of a croissant. 3D surface rendering verified the coiled turning and visualized, as expected, not a smooth but uneven myelin surface (Fig. 15b). Interestingly, the coiled myelin turns showed regular interspaces of 5.2 μm in average length (Fig. 15c). Ultra-structural analysis of OCS let us notice uncompact, outer myelin membrane layers, the myelin outer loop, that displayed helical turns along the internode, thus most likely accounting for the light microscopic observation of myelin helical turning (Fig. 15d, e).

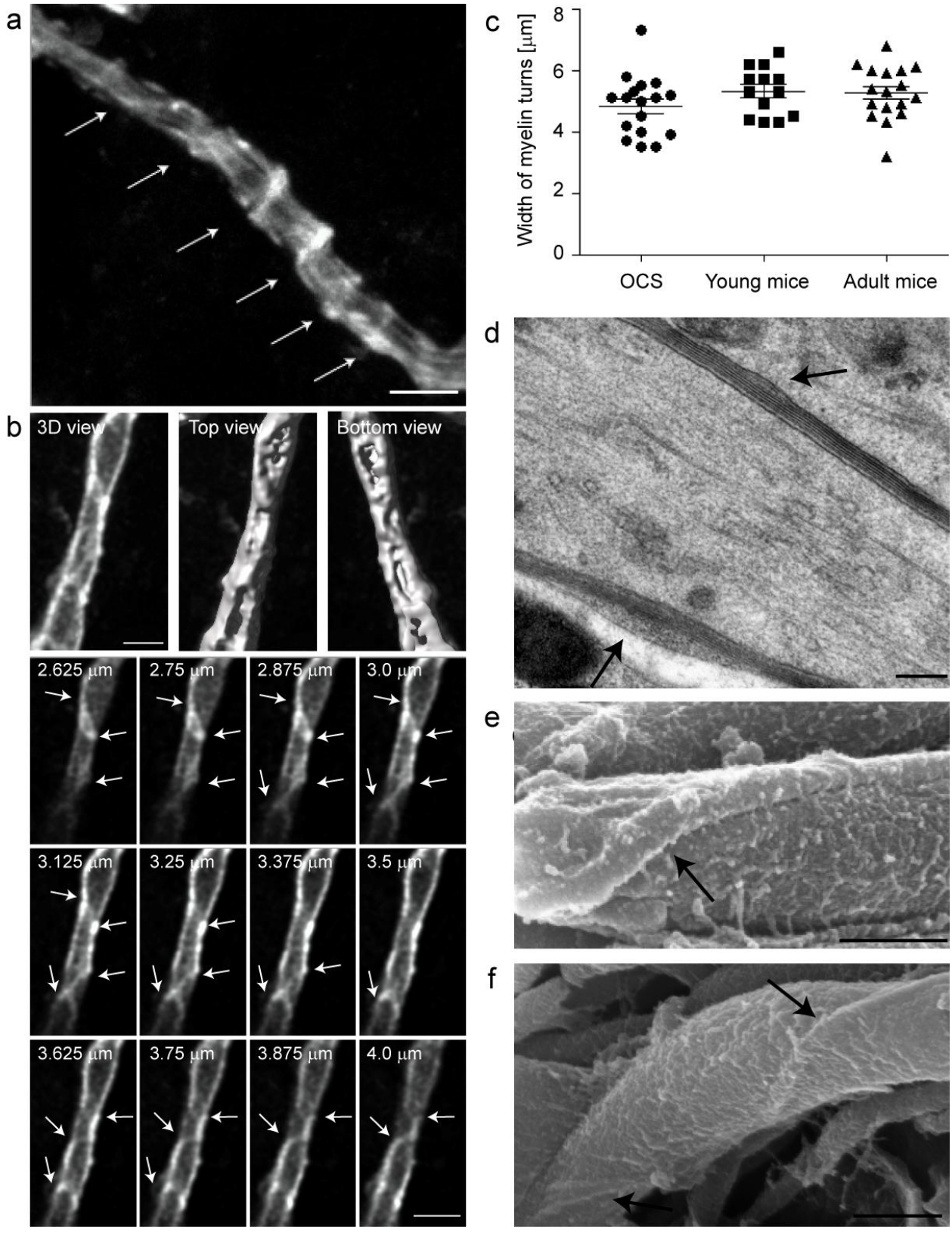
a
b
3D view
Top view
Bottom view
2.625 µm
2.75 µm
2.875 µm
3.0 µm
3.125 µm
3.25 µm
3.375 µm
3.5 µm
3.625 µm
3.75 µm
3.875 µm
4.0 µm
c
Width of myelin turns [µm]
0
2
4
6
8
OCS
Young mice
Adult mice
d
e
f

Fig. 15 **Coiled turning of myelin observed in light microscopy is evoked by the myelin outer loop**. (a, b) Confocal microscopic analysis of PLP-GFP (white) shows (a) coiled myelin with (c) similar spacing along the internode (arrows in a). Myelin coiling typically, but not exclusively ran (b) bi-directional as seen in the slice view (arrows). 3D surface rendering verified the coiled turning and visualized, as expected, not a smooth but uneven myelin surface. Transmission (d) and scanning (e, f) electron microscopy revealed turning of the cytoplasma containing outer loop. Scale bars equal in (a, b) 3 µm, in (c, d) 500 nm and in (e) 200 nm.

Likewise, we detected coiled myelin turns with similar characteristics in perfusion-fixed young and adult PLP-GFP (Fig. 16) and wildtype mice (not shown). This excluded not only any OCS or PLP-GFP related artefacts but demonstrated that the coiled turns of myelin represent the overall myelin structure in various regions in the CNS irrespective of the developmental stage.

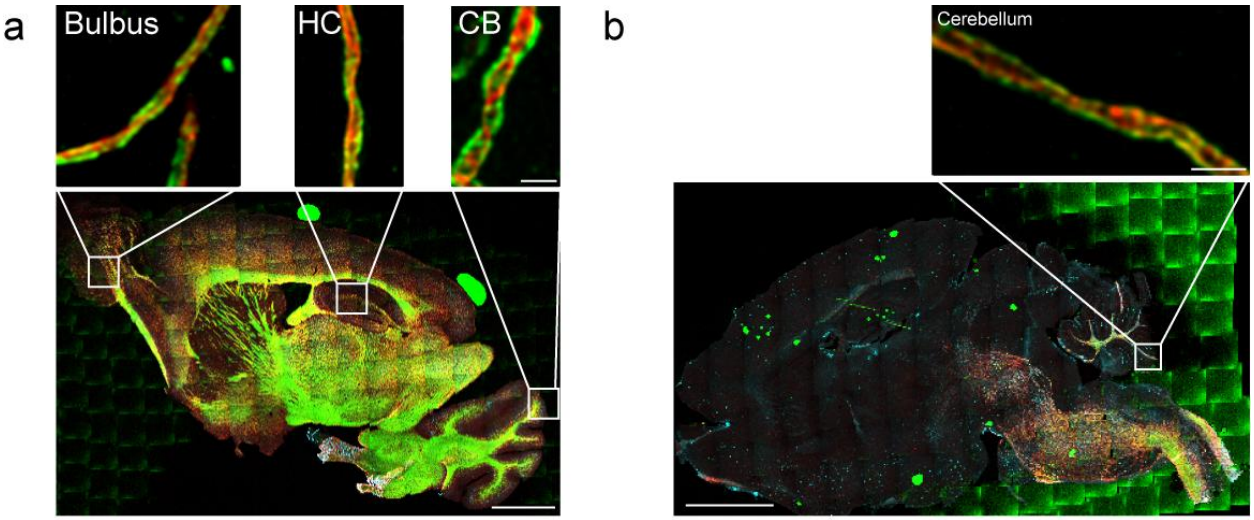

Fig. 16 **Similar myelin helix formation is found in different brain regions of young and adult mice**. Confocal microscopic tile scans of perfusion fixed adult (a) and young (b) PLP-GFP (green) mouse brains that were stitched and analyzed for MOG (red, in a) or MBP (red, in b). Even in the adult mouse, different brain regions reveal myelin turns similar to these found in OCS. HC = Hippocampus, CB = Cerebellum; scale bars equal in (a), (b) 1000 µm and for inserts 2 µm.

4.2.2 The myelin helix forms during myelin outgrowth and is highly motile

To profit from the moving image in understanding how the final myelin product is formed, we initially performed coarse time-lapse imaging and could observe myelin outgrowth in OCS over a distance of up to 40 µm (Fig. 17a). Subsequent high-resolution time-lapse imaging revealed live myelination with beginning myelin helix formation (Fig. 17b). Once the helix was formed, the myelin turning between the internodes appeared not to be fixed but rather to flow in an undulated manner (not shown).

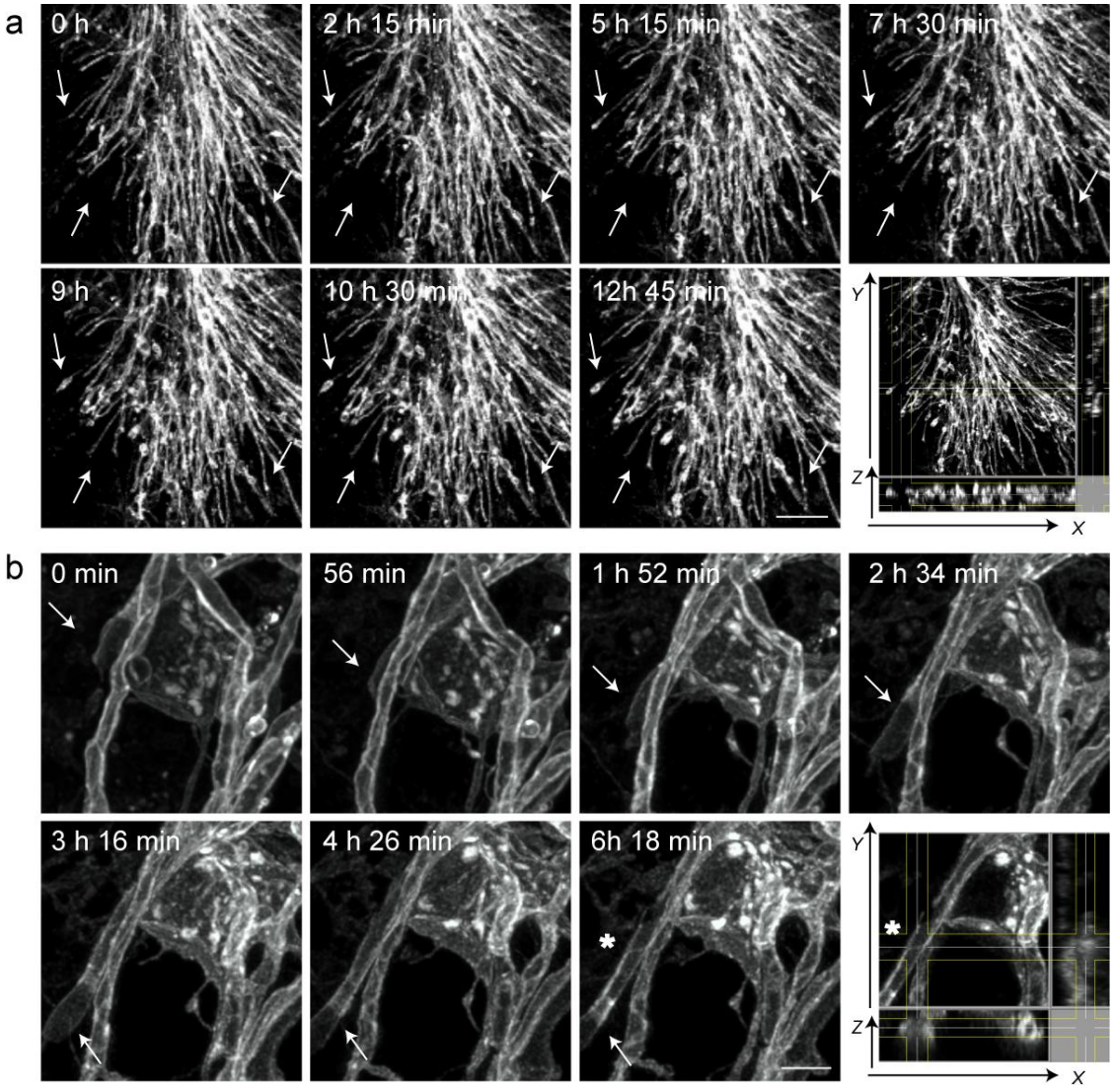

Fig. 17 **Live myelin outgrowth**. (a) Coarse confocal time lapse imaging of PLP-GFP (white) in OCS showed live myelination over a distance of up to 40 mm during the time imaged as indicated by arrows. (b) high-resolution confocal imaging revealed myelin helix formation (asterisk) during myelin outgrowth (arrows). (a and b right panel) Slice view of the respective confocal z-stacks confirmed stable slice position in the z-plane and excluded any z-shift related misinterpretations. Time elapsed after the start of imaging is shown in the left upper corner. Scale bars equal in (a) 50 μm and in (b) 3 μm.

4.2.3 The transition of OLG processes into myelin forms a triangular shape

The question of how myelin components actually reach the myelin sheath has been discussed for long. The thin OLG processes, which appear to merge into the insulating myelin sheath, have only seldom been shown by light microscopy, most likely due to resolution problems. In time-lapse imaging from OLG cell body and processes, we noticed within the process endosomal transport of PLP-GFP, suggesting liquid myelin "dough" or micelles being pumped from the OLG cell body into the myelin sheath (Fig. 18b). The transition from OLG process to myelin sheath could only be visualized by increased exposure and revealed in the slice view a triangular shape (Fig. 18a).

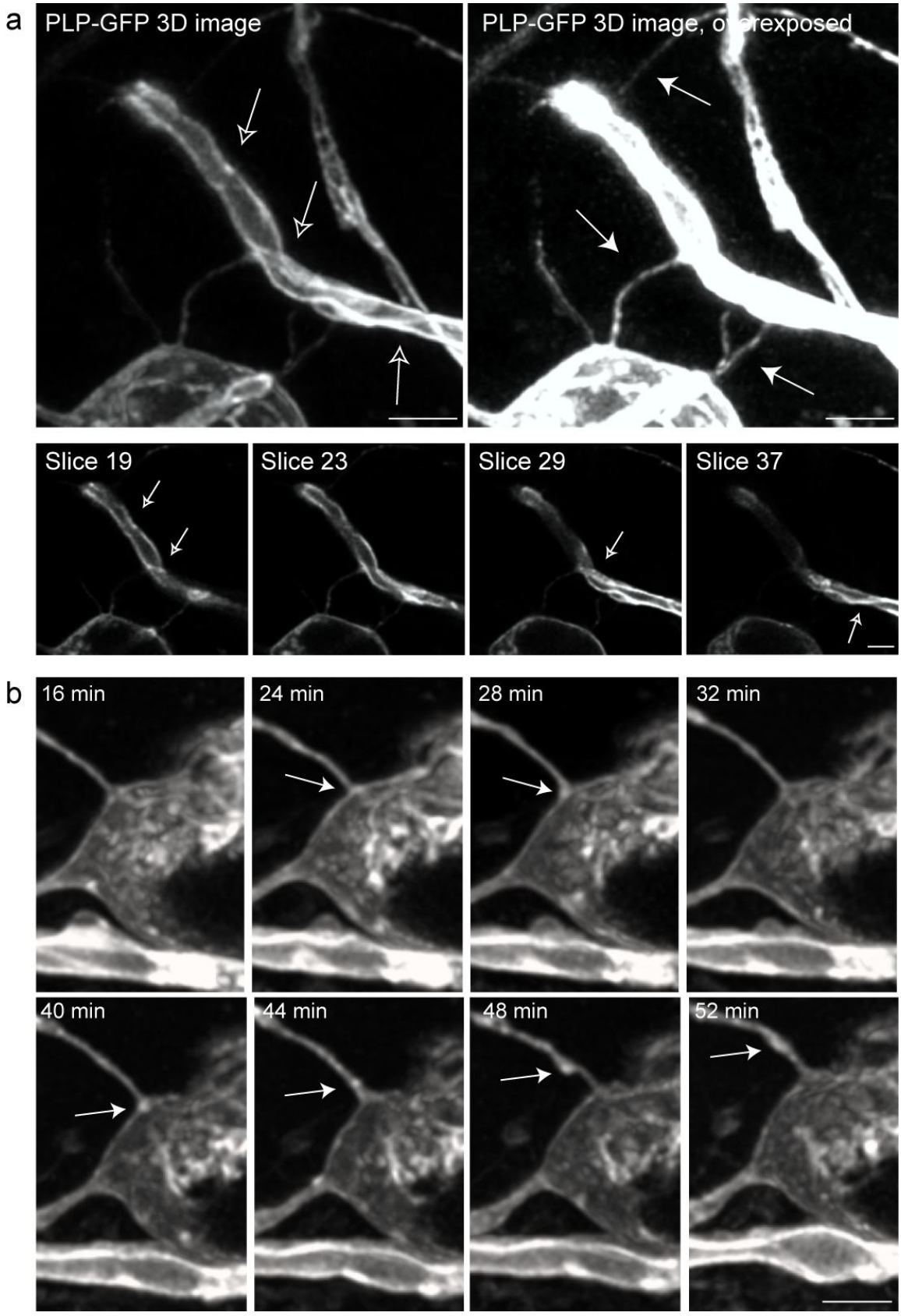
a
PLP-GFP 3D image
PLP-GFP 3D image, overexposed
Slice 19
Slice 23
Slice 29
Slice 37
b
16 min
24 min
28 min
32 min
40 min
44 min
48 min
52 min

Fig. 18 **Endosomal transport of PLP-GFP in OLG processes that open out in a triangular shape into myelin**. Increased exposure (a) revealed the rarely visualized transition from OLG processes to the myelin sheath forming a triangular shape, confirmed in the respective slice view (a). PLP-GFP endosomal transport within OLG processes was observed from the OLG cell body to the myelin by performing high-resolution confocal imaging. Time elapsed after the start of imaging is shown in the left upper corner. Scale bars equal 3 μm.

4.2.4 The "liquid croissant" model of myelination

As discussed above, the previous concepts fall short in explaining the formation of myelin ensheathment of CNS axons. As we detected an evenly spaced, bidirectional helical turning of myelin along the internode in OCS, young and adult mouse CNS irrespectively of the imaging method used, we here present our "liquid croissant" model (Fig. 19) in reference to the bi-directional dough edge spirals of a croissant: (1) myelin lipids/proteins are "poured out" through the OLG process like dough, which spreads sideward until it attaches to axonal cell adhesion molecules (CAM). (2) While this pouring process continues, axonal CAMs indirectly guide the wrapping by being associated with axonal motor proteins that move in a coordinated fashion around the axonal cytoskeleton, which results in the turning of the entire myelin/axonal CAMs complex. (3) Myelin thickening is thus achieved by new layers forming *on top* of the inner ones. (4) Since the second and subsequent layers originate from the "hose" which spreads in a triangular shape onto the layers below, two spiral formations turning in different orientations originate to left and right from the location where the "hose" enters the myelin sheath. These spirals, formed by laterally expanding surface myelin layers on the top of broader inner layers, resemble the dough edges visible on a "croissant".

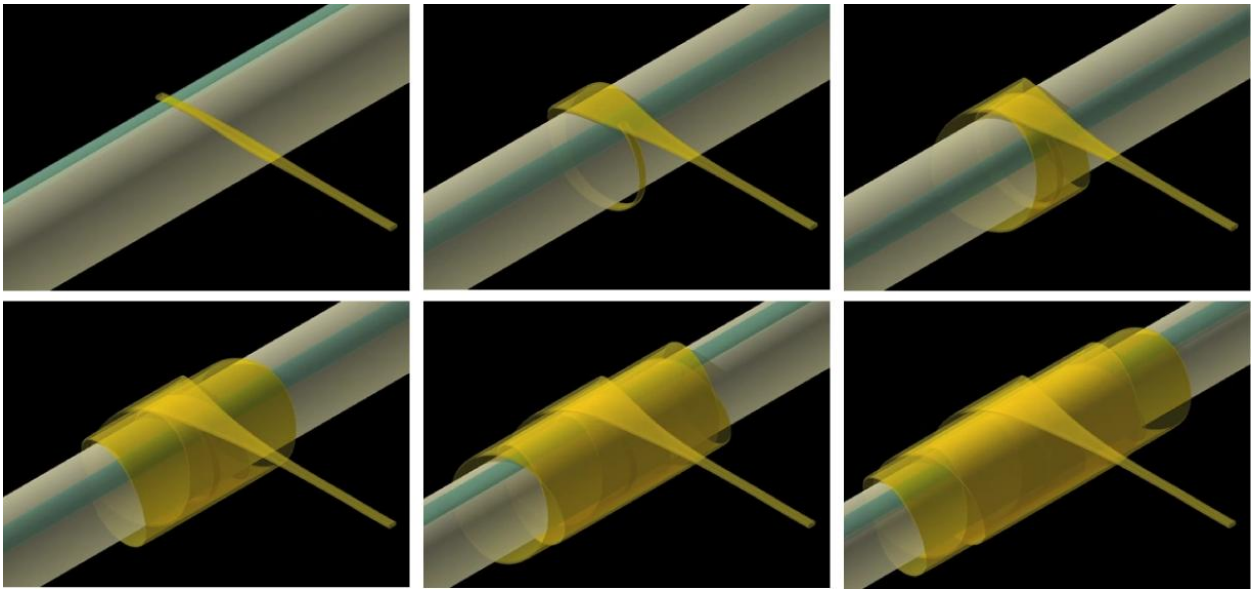

Fig. 19 **The "liquid croissant" model of myelination**. Based on our data and recent findings we propose that "poured out" myelin lipids/proteins (yellow) attach via the OLG process to axonal cell adhesion molecules (cyan). While this pouring process continues, axonal cell adhesion molecules indirectly guide the wrapping/spreading by being associated with axonal motor proteins that move in a coordinated fashion around the axonal cytoskeleton (turning of the cyan line while the myelin is wrapping around). New myelin layers form thus on top of the inner ones to achieve myelin thickening.

In conclusion, we hypothesize that the axon is actively involved and guides myelination. In our model, new myelin components are "poured" through the OLG process to form new layers *on top* of the inner ones. The proof of our scenario remains to be determined. Yet, this may represent one of the most complex problems in myelin research, especially with respect to the limited knowledge on the molecular events and interaction partners during active myelination in the CNS.

5 Discussion

5.1 The CD4/CD8 T cell misunderstanding in T cell-mediated autoimmunity

As discussed below, the role of CD8+ T cells in autoimmune research has only recently become subject of intense investigation. Despite elegant approaches that strengthen a CD8-mediated autoimmune pathogenesis, key questions in MS pathology, such as causes for axonal loss, the morphological equivalent to permanent neurological deficits, remained elusive. We have therefore investigated whether myelin-specific CD8+ T cells directly attack axons or whether axonal loss occurs as result of a targeted hit against myelinated structures indicating "collateral bystander damage" [109].

The turning point in understanding the importance of CD8+ T cells in autoimmune pathogenesis was not until recently. Up to then, the pathogenesis of autoimmune diseases was attributed either to CD4+ T cells like in MS, rheumatoid arthritis (RA) and diabetes mellitus (DM) type I or to B cells like in myasthenia gravis and systemic lupus erythematousus. The two major reasons for this were (1) a genetic association with HLA II alleles that present antigen to CD4+ T cells [35,110] and (2) the nature of the respective research tools like EAE, a CD4+ T cell-mediated disease [111]. However, not only show a variety of other autoimmune diseases (like ankylosing spondylitis, Behcet's disease, and psoriasis) an HLA I association [112] but emerging evidence, particularly in MS, has broken the ignorance towards CD8+ T cells by the autoimmune research community.

The preponderance of CD8+ T cells in MS lesions was overlooked for long, most likely due to the lack of anti-CD8 antibodies that would label in formalin fixed tissue [43]. However, the pathophysiological consequences of predominating CD8+ T cells in MS lesions [113,114] was clarified only later by work from Klaus Rajewsky's group. Sequencing of amplified TCR V-

regions by single cell PCR allowed the authors to detect particular gene rearrangements that derived in majority from CD8+ T cell clones but not CD4 + T cells present in MS lesions [42]. Subsequent complementarity-determining region 3 (CDR3) spectratyping revealed the persistence of these infiltrating CD8+ T cell clones in the CSF [44,115] and blood [44] of MS patients.

In parallel, the thus suspected pathogenic role of CD8+ T cells in MS was strengthened. For example, myelin-specific CD8+ T cells in the blood of MS patients appeared to proliferate in the presence of peptides from various myelin proteins [45,116]. Likewise, numbers of infiltrating CD8+ T cells could be correlated with the extent of axonal damage in MS lesions [117]. Complementary, MHC class I expression was claimed to be up-regulated in MS lesions on OLG and neurons [118]. However, small case numbers and insufficient immunostainings in the latter study leave MHC class I expression, especially on axons, questionable.

That myelin-specific CD8+ T cells can cause autoimmune damage was found in two independent experimental models. In one set-up, adoptively transferred MOG-specific CD8+ T cells from MOG_{35-55}/CFA-induced EAE animals prompted EAE like symptoms in WT or $RAG1^{-/-}$ recipient mice. Interestingly, the authors were unable to induce adoptive transfer EAE with these MOG-specific CD8+ T cells in MHC class II $^{-/-}$ deficient animals [49]. In the other approach, MBP-specific CD8+ T cells were isolated from $MBP^{-/-}$ or WT mice immunized with a previously identified peptide MBP_{79-87} [119]. Adoptive transfer of MBP-specific CD8+ T cells into WT or scid recipient mice resulted in fulminant EAE but was absent in $MBP^{-/-}$ mice [50].

However, in both studies only few CD8+ T cells infiltrated the brain. To study therefore CD8+ T cell CNS infiltration, CL4 mice, carrying CD8+ T cells with a transgenic TCR for the influenza virus hemagglutinin (HA) 512-520 antigen [120] received intrathecal injections of their cognate

antigen or the control peptide Cw3. An accumulation of HA-specific CD8+ T cells was only seen in case of the specific HA-antigen and was claimed to dependent on MHC class I expression by cerebral endothelium but not on perivascular macrophages that had been depleted by clodronate-loaded liposomes [121]. Although an endothelial contribution to T cell brain infiltration certainly exists [122], limiting this involvement solely to MHC class I expressing endothelium appears too simplified, especially as the "proof" relied on MHC class I antibody depletion only.

As the CD8+ T cell-mediated EAE models revealed demyelination that was associated with broad tissue damage reminiscent of ischemic injury, two independent groups used CD8+ T cells specific for a neo-self antigen restricted in its expression to OLG to investigate the direct impact of CD8+ T cells on myelin. In one approach, the authors generated $Rosa^{26tm(HA)1Libl}$ mice, in which the influenza virus hemagglutinin (HA) sequence was introduced in the ubiquitously active Rosa 26 locus flanked by a LoxP stop cassette. $Rosa^{26tm(HA)1Libl}$ mice were crossed with MOGi-Cre mice [123] to allow expression of HA solely in OLG (then referred to as DKI mice). Adoptive transfer of in-vitro stimulated and GFP labeled CD8+ T cells carrying a transgenic TCR for the $HA_{512-520}$ derived from CL4 transgenic mice [120] caused severe neurological symptoms in DKI but not in WT mice. Pathological analysis confirmed CD8+ T cell infiltrates in CNS lesions with demyelination [51]. In the other approach, the authors used transgenic ODC-OVA mice that express the neo-self antigen OVA solely in OLG [103]. Adoptive transfer of OT-I T cells in 2-week-old ODC-OVA x RAG-$1^{-/-}$ recipient mice resulted in spontaneous EAE by invading CD8+ T cells. The observed neurological symptoms were equally found in ODC-OVA x RAG-$1^{-/-}$ animals crossed with OT-I mice. Interestingly, in their set-up EAE occurred only in 2-week-old mice and was most pronounced in the RAG1-/- lymphopenic environment [52].

5.2 CD8+ T cell-mediated target cell death

Despite their elegancy, neither of the discussed studies addressed the direct impact of CD8+ T cells on CNS tissue damage and especially lacked the question in which fashion CD8+ T cells may contribute to axonal damage.

The key finding of our study was that "innocent" axons were damaged by an apparently imprecise targeting of myelin-specific CD8+ T cells. We proved this "collateral bystander damage" of axons by restricting cognate antigen expression to OLG, which appear to efficiently present peptides processed from endogenous protein to auto-aggressive cytotoxic CD8+ T cells. Later, our results that "collateral bystander damage" causes axonal loss were confirmed by others [124], raising the question towards the underlying mechanism leading to CD8-mediated neurotoxicity.

In general, CD8+ T cells only respond to their cognate peptide antigens (8–11 amino acids in length) when presented by MHC class I molecules [125]. In experimental models, MHC class I expression on OLG was shown in-vitro [47,126] and in-vivo [127] under inflammatory conditions. Likewise, we found that MHC class I expression on OLG was induced by IFNγ. However, MHC class I expression on neurons remains controversial. With the assumption that infected or damaged neurons reside in an inflammatory environment and have a disrupted electrical function, dissociated neurons were electrically silenced and treated with IFNγ. Only under these rather artificial conditions MHC class I expression could be detected [128]. In-vivo, inflammation with attenuated murine hepatitis virus caused MHC class I expression in the neuronal cytoplasm but not on dendrites or axons [127]. Yet, the neuron –specific enolase (NSE) marker used for neuron identification has been described to coincide with differentiating OLG [129] so that an

additional neuronal marker would have been desirable. As we could not formally exclude MHC class I expression on neurons, we challenged and verified our findings by incubating OCS with complete ovalbumin protein. We based this investigation on a hypothetical scenario, in which myelin proteins would be released by myelin damage. Subsequent extracellular digestion could potentially lead to loading of myelin protein derived peptides onto an accessible MHC class I positive cell, including axons, thus enabling CD8+ T cells to attack axons themselves. Yet, we could not detect any CD8-mediated axonal damage when mimicking myelin release by ovalbumin addition. Apparently, extracellular processing of complete 385 amino acid long ovalbumin protein specifically to the cognate SIINFEKL peptide is a rather rare event in OCS.

With respect to our observation that myelin and axons did not express MHC class II molecules as described previously [118], CNS tissue integrity in the presence of OT-II or 2D2 transgenic CD4+ T cells was expected. It is therefore remarkable that PLP-specific CD4+ T cells were claimed to induce CNS damage in a non-MHC class II restricted fashion [39]. Possible reasons explaining these controversial observations may be: (1) Nitsch *et al* employed acute hippocampal brain slices from SJL/J mice, a strain known to be more susceptible to CD4-mediated EAE than the C57BL/6 (B6) mice we used; (2) Long-term cultures and re-stimulation of antigen specific CD4+ T cells is known to select for a T cell phenotype acquiring lymphokine-activated killer (LAK) properties [130] reminding of NK cells [131]; (3) CD4+ T cell-mediated neuronal damage was claimed by changes in cellular calcium concentrations, visualized by the cell-permeable Ca^{2+}-indicator Fluo-4, which is however not proof of axonal damage. As such, most likely the different experimental set-ups and read-outs account for the controversial finding.

The mechanisms which may cause axonal damage by CD8+ T cells appear not entirely clear yet. As discussed below, not the mere presence of CD8+ T cells but the integration of different signals, like TCR signaling, chemokine pattern and type of employed CD8+ T cell appear to decide on the outcome of CD8+ T cell effector functions. Recently, for example, the paradox was clarified how apparently healthy neurons latently infected by herpes simplex virus (HSV)-1 can be surrounded by CD8+ T cells without being damaged. In their study, the authors found that CD8+ T cells selectively cleared virus without killing infected neurons by employing non-lytic mechanisms like release of IFNγ but majorly by the direct proteolytic activity of granzyme B [132]. In turn, in the model of acute viral meningoencephalitis, CD8+ T cells were found to chemoattract monocytes and myelocytes, which then cause CNS damage [133].

In the classic view, CD8+ T cells form an immune synapse with their target cell upon recognition [134]. This may occur even at low numbers of antigen-presenting MHC class I molecules on the target cell, in our case OLG [135]. In the next step, both high- and low-avidity MHC class I-TCR interactions lead to centrosome polarization, yet only high-avidity interactions increase TCR signaling that recruits lytic granules to the polarized centrosome [136]. The subsequent polarized release of lytic granules is thought to spare surrounding tissue. We also found polarization of lytic granules but observed collateral bystander damage of axons. This raises the question whether myelin and axon are too closely engaged to kill the one and spare the other or if our observation was related to the CD8+ T cells used.

We previously observed that anti-MOG antibody together with complement could induce a demyelination in slices without damaging axons [137], which appears in comparison with a CD8-mediated damage rather targeted. T cells carrying transgenic TCRs are often criticized for that they may not accurately model endogenous T cell responses. We used OT-I transgenic T cells

that were originally selected and subcloned from CTLs derived from OVA-immunized B6 mice [138]. Based on their TCR identity, OT-I transgenic mice were then generated carrying these SIINFEKL-specific CD8+ T cells [139]. As other TCR transgenic strains, OT-I mice hold unphysiological numbers of CD8+ T cells expressing the transgenic OVA TCR and are strongly cytolytic towards OVA-expressing target cells [139,140], even in the absence of classical co-stimulatory molecules like CD80/86 [52]. Therefore, the choice of OT-I CD8+ T cells may have influenced our findings. Yet, the lack of alternative CD8+ T cells tools appears to justify their broad use in autoimmune research and may still be indicative for further understanding.

5.3 Axonal molecules that initiate and regulate myelination

A growing number of observations points to a prominent role of axons in proper myelination and myelin maintenance [141]. Accordingly, myelination is thought to be orchestrated by the balance of stimulating and inhibitory axonal factors that can be either expressed on the axonal surface or represent soluble mediators [142].

The first evidence that rather axonal signals than an intrinsic myelination program of the glial cell regulates myelination came from the pioneer studies by Aguayo *et al*. The authors observed that Schwann cells were able to make myelin in the presence of a regenerating nerve, although they had not made any myelin before [143]. While oligodendrocyte precursor cells (OPC) can proliferate and differentiate into postmitotic OLG in neuron-free cultures [144], specific axonal signals for proper OLG myelin formation are required. For example, the ratio of axon diameter to myelin thickness (called g-ratio) was shown to remain constant [145]. Similarly, OLG that had only been myelinating small caliber optic nerve fibers, were demonstrated to form proper size-adjusted myelin sheaths, when transplanted to larger spinal cord axons [146] or when the axon

caliber was reduced [147]. Likewise, under healthy conditions previously unmyelinated CNS axons retain their ability to become myelinated as shown by myelination of retinal axons after transplantation of CG-4 cells, an OPC cell line [148]. Furthermore, specific recognition molecules on the axonal surface seem to be pivotal, as OLG form true, spirally wrapped myelin sheaths in-vitro solely around axons but not dendrites [149].

Despite this clear axonal influence on myelination, only little is known about the exact underlying mechanisms, especially in the CNS. Up to date, type III neuregulin-1 (NRG1) expressed on axons is the only identified molecule that was shown to determine both myelin formation [150] and myelin sheath thickness [151] in the PNS. Yet, its role in the CNS is clearly distinct, as NRG1 deficient mice lack any CNS phenotype [152]. Regarding myelin maintenance, cellular prion protein (PrP^{c}) expressed by neurons was recently implied to play an essential role in the PNS, while its function in the CNS remains less clear given myelin integrity in *Prnp*$^{o/o}$ mice [153] . Apart from that, a few axonal-glial interaction partners were suggested to influence myelination. Laminin-2 was proposed to interact with an OLG integrin, based on the observations that (1) OLG produce increased myelin sheaths when cultured on laminin-2 [154], (2) laminin-2 absence causes dysmyelination in mice [155] and humans [156] and (3) antibody-blocking experiments [157] or OLG deficient for β1 integrin display decreased-absent myelination [158]. Recently, OLG contactin, a glycosylphosphatidylinositol (GPI)-anchored CAM of the Ig family was proposed to interact with the axonal CAM L1 that signals together with the OLG integrin/ axonal laminin-2 complex through Fyn activation [159].

Moreover, axonal binding partners can also inhibit myelination. The axonal polysialted neural cell adhesion molecule (PSA-NCAM) was observed to correlate inversely with the myelin sheath thickness in-vivo [160], to be down-regulated by the onset of myelination [161] and to be up-regulated

during demyelination in-vitro [162]. Likewise, Notch1 expressed by OLG [163] was described in-vitro and in-vivo to bind to its ligand Jagged 1, which is expressed by axons to inhibit OPC differentiation [164] and OLG myelination [165].

Taken together, only a few axonal-glial interaction partners and mechanisms are known and future studies are needed to better understand the structural and molecular changes in axon and OLG during myelination.

5.4 Indications that axonal energy is required for myelination

Clearly, energy has to be consumed in order that myelin can achieve its sophisticated cytoarchitecture, a fact that has not thoroughly been investigated up to this date. In-vitro, OLG processes were claimed to contain mitochondria [166] but not a single EM study has described conclusively mitochondria within the growing myelin inner loop. This lack of evidence is not surprising given the relatively large-sized mitochondria that would have to fit in the small cytoplasmic inclusions of the inner loop. Yet, the energy source for myelination remains elusive. In this context, ATP could formally (1) diffuse over long distance from the OLG cell body through the process to the growing part, a rather rare event [167], (2) be taken up from an extracellular source although ATP then serves paracrine signaling in general [168] or (3) ATP could be produced and consumed within the axon for myelination to occur.

Several recent findings indirectly support the latter possibility by approving an axonal support in myelination that goes beyond simple adhesion. For example, only pseudomyelin structures that lack the tight compact characteristic of proper myelin, were described to form around PFA-fixated, thus dead, axons [169], which are similarly observed without co-cultured axons [170] or in the presence of carbon fibers [171]. While this undoubtedly demonstrates an intrinsic myelin formation

program within the OLG, it implicates that more is required than simple axonal recognition signals for proper myelination to occur. In line, only healthy axons that activity-dependently release ATP become myelinated [172], whereas blockage of axonal activity with the sodium channel-specific neurotoxin tetrodotoxin (TTX) inhibits myelination [173]. Recently, axonal mitochondria were described to change size and distribution dependent on the demyelination or remyelination status [174]. That an active axonal process in myelination may be needed for myelination is further supported by studies of the major kinesin motor protein in the CNS, KIF1B, which is involved in axonal transport of mitochondria and synaptic vesicles [175]. Its impairment was associated with hypomyelination and Charcot-Marie-Tooth disease type II [176] and is discussed in MS susceptibility [177], an astonishing finding with respect to a primary dysfunction within the axon that should theoretically not affect myelination per se.

Besides a potential function as energy source, we propose that the axon may directly guide outpoured myelin along the internode by molecules like the axonal cell adhesion molecules caspr (contactin-associated protein) [178,179] and contactin which interact with glial neurofascin (NF) 155 [180]. Accordingly, caspr was described to bind with its cytoplasmic domain to protein 4.1 [178], which in turn binds to the axonal actin skeleton [181]. In addition, mice lacking either caspr [182] or contactin [87] fail to assemble myelin properly, most pronouncedly observed at the paranode. Furthermore, caspr is initially homogenously distributed along the axon and achieves its characteristic helical pattern only upon myelination [179], which was previously suggested to mirror myelination [98]. Moreover, we believe that our hypothesis is also in favor from an evolutionary point of view, as axons apparently depend more on myelination [63] than the myelinating cell on the axon.

5.5 Developmental myelination versus remyelination

Various aspects closely connect the understanding of myelin formation with the pathological state of demyelination and its regenerative process, remyelination. Remyelination is thought to mainly influence the outcome of demyelinating diseases, such as MS and is therefore intensely studied. In theory, similar mechanisms to those described for developmental myelination could take place for remyelination. Yet, the past decades of remyelination research were dedicated to the clarification whether remyelination occurs from surviving OLG that regenerate their "just" lost processes and myelin sheaths or from invading progenitor cells that differentiate into remyelinating OLG. As discussed below, up to date neither possibility has been truly resolved and in addition, the main molecular similarities and differences between developmental myelin formation and remyelination remain elusive.

In the CNS, the loss of myelin is usually the result of primary and not secondary demyelination, in which myelin degenerates as consequence of primary axonal loss. Primary demyelination is either caused by genetic abnormalities within OLG (like leukodystrophies) or - in terms of morbidity more significant - by an inflammatory damage of myelin/OLG (like in MS). Regardless of the cause, the loss of myelin results in an acute conduction block that is resolved by an even distribution of Na^+ channels to allow non-saltatory conduction along the demyelinated internode [183]. This deficit can be solved by remyelination, which restores the myelin sheath and thus repairs saltatory conduction and functional deficits. Interestingly, the original dimensions of myelination are not entirely reestablished during remyelination showing a thinner and shorter myelin sheath than expected [184,185], making remyelinated lesions appear less intense with myelin stains (so-called "shadow plaques").

The models in which demyelination is induced to study remyelination typically employ toxins, like dietary cuprizone or injected lysolecithin, traumatic injury, viral infections or immune-mediated mechanisms like in EAE [186]. Using these models, only a few differences between developmental myelination and remyelination have been elucidated. For example, the transcription factor OLIG1 is thought to be essential for developmental myelination but appears to play a redundant role in OPC differentiation during remyelination [187]. Likewise, conditional *NOTCH1* knockout from OPC did not influence remyelination [188] while Notch receptor activation inhibits OLG differentiation during myelination as discussed above. Despite different pathoetiologies in the classic demyelination models, certain key features appear to be shared.

Firstly, axonal survival is indispensible for remyelination. Environmental mediators may cause however secondary axonal damage of the "naked" axon. Demyelinated axons were described to suffer from disturbed mitochondrial function, pathological Na^+ influx which subsequently causes Ca^{2+} influx [189] which in turn activates intra-axonal proteases resulting in neurofilament breakdown and perturbation of axonal transport [190] and integrity [191]. In addition, the demyelinated axon is implicated itself in inhibiting remyelination by expressing PSA-NCAM [162] (as discussed above) or LINGO-1 (Nogo-receptor interacting protein) which inhibits myelination by interacting with the Nogo receptor complex. The disruption of LINGO-1 promotes OPC differentiation and OLG myelination independent of axonal caliber [192]. In view of our hypothesis and the few identified axo-glial interaction partners discussed above, it is intriguing to speculate that compromised remyelination could result from impaired axons that have undergone too dramatic intrinsic changes to recruit OPC (see below) and direct remyelination.

Secondly, the currently most accepted and compelling notion suggests that adult OPC [193] migrate to demyelinated areas, similarly to the process during developmental myelination [194] and

differentiate into myelinating OLG [195]. OPC are commonly identified by – the not exclusive - expression of proteoglycan NG2, platelet-derived growth factor receptor-α (PDGFRα) or the transcription factor OLIG1 [196]. Yet, all evidences for an OPC involvement in remyelination remain indirect: (1) autoradiographic tracing has identified dividing cells that give rise to myelinating OLG but these cells were not proven to be OPCs [197], (2) transplanted OPCs were shown to remyelinate demyelinated areas [198,199], (3) OPCs repopulate demyelinated areas before new OLG appear [200] and (4) the failure of remyelination was associated with an age-dependent decrease in OPC recruitment and differentiation [201]. In contrast, the migration of post-mitotic OLG to a demyelinated area seems unlikely and even their local participation was negated. However, both studies carried major caveats as they employed OLG, which had either been subjected to a high dose of X-ray radiation [202] or were maintained in-vitro [203], both conditions that are likely to cause disturbances in cell function. As such, remyelination may recapitulate certain features of developmental myelination but deeper insight into cellular and molecular mechanisms or axo-glial interaction partners is needed to conclusively understand this regenerative process.

5.6 Concluding remark

We here presented two important findings with respect to CNS (patho)physiological events. Fully aware that the outlined CD8+ T cell scenario is most likely not the only relevant mechanism of CNS tissue damage in inflammatory CNS diseases, we are confident that our findings critically contribute to the understanding of CD8-mediated neuropathology in CNS inflammation, strengthen a pathogenic role of CD8+ T cells in MS and advocate for the development of future immunotherapies aiming at the CD8-myelin/OLG interface. In addition, we are convinced that the “liquid croissant” model describing fluid myelin to be guided by an energy consuming process within the axon to achieve myelination, reshapes the current understanding of myelin formation and may explain myelination deficits in remyelination and axonopathies.

Abbreviations

APC	antigen presenting cell
Caspr	contactin-associated protein
CD	cluster of differentiation
CNS	central nervous system
CSF	cerebrospinal fluid
DM	diabetes mellitus
EAE	experimental autoimmune encephalomyelitis
(E)GFP	(enhanced) green fluorescent protein
HLA	human leukocyte antigen
IFN	interferon
Ig	immunoglobulin
LM	light microscopy
MBP	myelin basic protein
MHC	major histocompatibility complex
MOG	myelin/oligodendrocyte glycoprotein
MS	multiple sclerosis
NG2	chondroitin sulfate proteoglycan NG2
NF	Neurofilament
OCS	organotypic cerebellar slice culture
OLG	oligodendrocyte
OPC	oligodendrocyte precursor cell
PLP	proteolipid protein
PSA-NCAM	Polysilyated- neural cell adhesion molecule
RA	rheumatoid arthritis
RT	room temperature
SEM	scanning electron microscopy
TCR	T cell receptor
TEM	transmission electron microscopy

Curriculum Vitae

Anna Bettina SOBOTTKA, MD

Born 1st of February 1980 in Frankfurt/Main, Germany; Nationality: German

Education

2007-2010	PhD thesis in the group of Prof. N. Goebels and Prof. B. Becher, Clinical and Experimental Neuroimmunology, University of Zurich, Switzerland (employed as PhD student at the University of Zurich since 10/2007)
2006-2007	Research fellow in Preclinical CNS Research at the F. Hoffmann-La Roche AG, Basel, Switzerland
09/2006	Medical Doctor (MD) from Charité, Humboldt-University, Berlin, Germany; MD thesis "Regulation of erythropoietin expression in renal cancer and primary established cell lines thereof" in the group of Prof. K.-U. Eckardt, University of Erlangen, Germany
05/2006	Licence to practise medicine (Approbation)
11/2005	Third State Examination; Completion of Medical Studies, Albert-Ludwigs-University, Freiburg, Germany
1999-2005	Study of Medicine at Charité, Humboldt University, Berlin (1999-2003) and at Albert-Ludwigs-University, Freiburg (2003-2005), Germany
06/1999	High School Graduation Diploma (Abitur), Heinrich-von-Gagern Gymnasium (Classical Secondary School), Frankfurt, Germany
1996-1997	Lyndon Institute, Lyndonville, Vermont, USA

Academic Honours and Awards

2009	Biogen-Dompé Research Award (together with N. Goebels)
2004	Scholarship of Baden-Württemberg (Federal State of Germany), Germany
2002	German National Academic Foundation (Studienstiftung des Deutschen Volkes)

Publications

Sobottka B, Ziegler U, Kaech A, Becher B, Goebels N. CNS live imaging implies a new mechanism of myelination: The liquid croissant model (manuscript in preparation)

Locatelli G*, Wörtge S*, Buch T*, Ingold B[+], Frommer F[+], **Sobottka B**, Bühlmann C, Bechmann I, Heppner FL, Waisman A[#], Becher B[#]. Induced oligodendrocyte death does not elicit anti-CNS immunity (Submitted to *Nat. Neuroscience*)

Metzger F, Staudenmaier C, Sänger S, van der Poel C, Sajid W, **Sobottka B**, Schuler A, Sawitzky M, Poirier R, Tuerck D, Schick E, Schaubmar A, Hesse F, Amrein K, Loetscher H, De Meyts P, Lynch GS, Hoeflich A, Schoenfeld H-J. Separation of fast from slow anabolism by site-specific PEGylation of insulin-like growth factor I. (Submitted to *JBC*)

Sobottka B, Harrer MD, Ziegler U, Fischer K, Wiendl H, Hünig T, Becher B, Goebels N. Collateral bystander damage by myelin-directed CD8+ T cells causes axonal loss. *Am J Pathol*. 2009 Sep;175(3):1160-6

Sobottka B, Reinhard D, Brockhaus M, Jacobsen H, and Metzger F. ProNGF inhibits NGF-mediated TrkA activation in PC12 cells. *J Neurochem*. 2008 Dec;107(5):1294-303

Wiesener MS, Münchenhagen P, Gläser M, **Sobottka B**, Knaup KX, Jozefowski K, Jürgensen JS, Roigas J, Warnecke C, Gröne HJ, Maxwell PH, Willam C, and Eckardt KU. Erythropoietin gene expression in renal carcinoma is considerably more frequent than paraneoplastic polycythemia. *Int J Cancer*. 2007 Dec 1;121(11):2434-42

*,[#] and [+]= these authors contributed equally

Acknowledgements

I am thankful to Norbert Goebels for the opportunity of doing my MD/PhD studies in his research group and I thank Burkhard Becher for welcoming me in his group after Norbert's move to Düsseldorf. I am grateful to both Norbert Goebels and Burkhard Becher for the independency and freedom of action during my MD/PhD. I thank my thesis committee members Sebastian Jessberger and Adriano Aguzzi for their support and helpful discussion. I thank Urs Ziegler, Andres Kaech and the members of the ZMB for conveying their passion for microscopy to me, their continuous endorsement and helpful advice. I thank the former Goebels, the Becher, Münz, Lünemann and Fontana group for the friendly and fun research environment.

Lastly, I thank particularly Angelo Brillout and my parents for their emotional support during my PhD studies. Their confidence and encouragement significantly contributed to the successful realization of this thesis.

References

1. Noseworthy, J.H., Lucchinetti, C., Rodriguez, M. & Weinshenker, B.G. Multiple sclerosis. *N Engl J Med* **343**, 938-952 (2000).
2. Franklin, R.J. & Ffrench-Constant, C. Remyelination in the CNS: from biology to therapy. *Nat Rev Neurosci* **9**, 839-855 (2008).
3. Lublin, F.D. The diagnosis of multiple sclerosis. *Curr Opin Neurol* **15**, 253-256 (2002).
4. Lassmann, H., Bruck, W. & Lucchinetti, C. Heterogeneity of multiple sclerosis pathogenesis: implications for diagnosis and therapy. *Trends Mol Med* **7**, 115-121 (2001).
5. Steinman, L. Multiple sclerosis: a two-stage disease. *Nat Immunol* **2**, 762-764 (2001).
6. Frohman, E.M., Racke, M.K. & Raine, C.S. Multiple sclerosis--the plaque and its pathogenesis. *N Engl J Med* **354**, 942-955 (2006).
7. Liblau, R.S., Wong, F.S., Mars, L.T. & Santamaria, P. Autoreactive CD8 T cells in organ-specific autoimmunity: emerging targets for therapeutic intervention. *Immunity* **17**, 1-6 (2002).
8. Medzhitov, R. & Janeway, C.A., Jr. Innate immunity: impact on the adaptive immune response. *Curr Opin Immunol* **9**, 4-9 (1997).
9. Beutler, B. Innate immunity: an overview. *Mol Immunol* **40**, 845-859 (2004).
10. Janeway, C.A., Jr. & Medzhitov, R. Innate immune recognition. *Annu Rev Immunol* **20**, 197-216 (2002).
11. Drickamer, K. & Taylor, M.E. Biology of animal lectins. *Annu Rev Cell Biol* **9**, 237-264 (1993).
12. Du Clos, T.W. & Mold, C. C-reactive protein: an activator of innate immunity and a modulator of adaptive immunity. *Immunol Res* **30**, 261-277 (2004).
13. Kohl, J. The role of complement in danger sensing and transmission. *Immunol Res* **34**, 157-176 (2006).
14. Peiser, L., Mukhopadhyay, S. & Gordon, S. Scavenger receptors in innate immunity. *Curr Opin Immunol* **14**, 123-128 (2002).
15. Takeda, K., Kaisho, T. & Akira, S. Toll-like receptors. *Annu Rev Immunol* **21**, 335-376 (2003).
16. Starr, T.K., Jameson, S.C. & Hogquist, K.A. Positive and negative selection of T cells. *Annu Rev Immunol* **21**, 139-176 (2003).
17. Kyewski, B. & Derbinski, J. Self-representation in the thymus: an extended view. *Nat Rev Immunol* **4**, 688-698 (2004).
18. Nemazee, D. & Hogquist, K.A. Antigen receptor selection by editing or downregulation of V(D)J recombination. *Curr Opin Immunol* **15**, 182-189 (2003).
19. Sakaguchi, S. Naturally arising CD4+ regulatory t cells for immunologic self-tolerance and negative control of immune responses. *Annu Rev Immunol* **22**, 531-562 (2004).
20. Walker, L.S. & Abbas, A.K. The enemy within: keeping self-reactive T cells at bay in the periphery. *Nat Rev Immunol* **2**, 11-19 (2002).
21. Pette, M., *et al.* Myelin basic protein-specific T lymphocyte lines from MS patients and healthy individuals. *Neurology* **40**, 1770-1776 (1990).
22. Zinkernagel, R.M. & Doherty, P.C. Restriction of in vitro T cell-mediated cytotoxicity in lymphocytic choriomeningitis within a syngeneic or semiallogeneic system. *Nature* **248**, 701-702 (1974).

23. O'Garra, A. & Robinson, D. Development and function of T helper 1 cells. *Adv Immunol* **83**, 133-162 (2004).
24. Dong, C. TH17 cells in development: an updated view of their molecular identity and genetic programming. *Nat Rev Immunol* **8**, 337-348 (2008).
25. Wan, Y.Y. Multi-tasking of helper T cells. *Immunology* **130**, 166-171 (2010).
26. Bevan, M.J. Helping the CD8(+) T-cell response. *Nat Rev Immunol* **4**, 595-602 (2004).
27. Trapani, J.A. & Smyth, M.J. Functional significance of the perforin/granzyme cell death pathway. *Nat Rev Immunol* **2**, 735-747 (2002).
28. Rioux, J.D. & Abbas, A.K. Paths to understanding the genetic basis of autoimmune disease. *Nature* **435**, 584-589 (2005).
29. Bjorses, P., Aaltonen, J., Horelli-Kuitunen, N., Yaspo, M.L. & Peltonen, L. Gene defect behind APECED: a new clue to autoimmunity. *Hum Mol Genet* **7**, 1547-1553 (1998).
30. Anderson, M.S., *et al.* Projection of an immunological self shadow within the thymus by the aire protein. *Science* **298**, 1395-1401 (2002).
31. Liston, A., Lesage, S., Wilson, J., Peltonen, L. & Goodnow, C.C. Aire regulates negative selection of organ-specific T cells. *Nat Immunol* **4**, 350-354 (2003).
32. Goodnow, C.C. Balancing immunity and tolerance: deleting and tuning lymphocyte repertoires. *Proc Natl Acad Sci U S A* **93**, 2264-2271 (1996).
33. Albert, L.J. & Inman, R.D. Molecular mimicry and autoimmunity. *N Engl J Med* **341**, 2068-2074 (1999).
34. O'Shea, J.J., Ma, A. & Lipsky, P. Cytokines and autoimmunity. *Nat Rev Immunol* **2**, 37-45 (2002).
35. Olerup, O. & Hillert, J. HLA class II-associated genetic susceptibility in multiple sclerosis: a critical evaluation. *Tissue Antigens* **38**, 1-15 (1991).
36. Madsen, L.S., *et al.* A humanized model for multiple sclerosis using HLA-DR2 and a human T-cell receptor. *Nat Genet* **23**, 343-347 (1999).
37. Zamvil, S.S. & Steinman, L. The T lymphocyte in experimental allergic encephalomyelitis. *Annu Rev Immunol* **8**, 579-621 (1990).
38. Gimsa, U., Peter, S.V., Lehmann, K., Bechmann, I. & Nitsch, R. Axonal damage induced by invading T cells in organotypic central nervous system tissue in vitro: involvement of microglial cells. *Brain Pathol* **10**, 365-377 (2000).
39. Nitsch, R., *et al.* Direct impact of T cells on neurons revealed by two-photon microscopy in living brain tissue. *J Neurosci* **24**, 2458-2464 (2004).
40. van Oosten, B.W., *et al.* Treatment of multiple sclerosis with the monoclonal anti-CD4 antibody cM-T412: results of a randomized, double-blind, placebo-controlled, MR-monitored phase II trial. *Neurology* **49**, 351-357 (1997).
41. Friese, M.A. & Fugger, L. Autoreactive CD8+ T cells in multiple sclerosis: a new target for therapy? *Brain* **128**, 1747-1763 (2005).
42. Babbe, H., *et al.* Clonal expansions of CD8(+) T cells dominate the T cell infiltrate in active multiple sclerosis lesions as shown by micromanipulation and single cell polymerase chain reaction. *J Exp Med* **192**, 393-404 (2000).
43. Neumann, H., Medana, I.M., Bauer, J. & Lassmann, H. Cytotoxic T lymphocytes in autoimmune and degenerative CNS diseases. *Trends Neurosci* **25**, 313-319 (2002).
44. Skulina, C., *et al.* Multiple sclerosis: brain-infiltrating CD8+ T cells persist as clonal expansions in the cerebrospinal fluid and blood. *Proc Natl Acad Sci U S A* **101**, 2428-2433 (2004).

45. Crawford, M.P., *et al.* High prevalence of autoreactive, neuroantigen-specific CD8+ T cells in multiple sclerosis revealed by novel flow cytometric assay. *Blood* **103**, 4222-4231 (2004).
46. Coles, A.J., *et al.* The window of therapeutic opportunity in multiple sclerosis: evidence from monoclonal antibody therapy. *J Neurol* **253**, 98-108 (2006).
47. Jurewicz, A., Biddison, W.E. & Antel, J.P. MHC class I-restricted lysis of human oligodendrocytes by myelin basic protein peptide-specific CD8 T lymphocytes. *J Immunol* **160**, 3056-3059 (1998).
48. Medana, I., Martinic, M.A., Wekerle, H. & Neumann, H. Transection of major histocompatibility complex class I-induced neurites by cytotoxic T lymphocytes. *Am J Pathol* **159**, 809-815 (2001).
49. Sun, D., *et al.* Myelin antigen-specific CD8+ T cells are encephalitogenic and produce severe disease in C57BL/6 mice. *J Immunol* **166**, 7579-7587 (2001).
50. Huseby, E.S., *et al.* A pathogenic role for myelin-specific CD8(+) T cells in a model for multiple sclerosis. *J Exp Med* **194**, 669-676 (2001).
51. Saxena, A., *et al.* Cutting edge: Multiple sclerosis-like lesions induced by effector CD8 T cells recognizing a sequestered antigen on oligodendrocytes. *J Immunol* **181**, 1617-1621 (2008).
52. Na, S.Y., *et al.* Naive CD8 T-cells initiate spontaneous autoimmunity to a sequestered model antigen of the central nervous system. *Brain* **131**, 2353-2365 (2008).
53. Baxter, A.G. The origin and application of experimental autoimmune encephalomyelitis. *Nat Rev Immunol* **7**, 904-912 (2007).
54. Barker, C.F. & Billingham, R.E. Immunologically privileged sites. *Adv Immunol* **25**, 1-54 (1977).
55. Abbott, N.J., Ronnback, L. & Hansson, E. Astrocyte-endothelial interactions at the blood-brain barrier. *Nat Rev Neurosci* **7**, 41-53 (2006).
56. Ransohoff, R.M., Kivisakk, P. & Kidd, G. Three or more routes for leukocyte migration into the central nervous system. *Nat Rev Immunol* **3**, 569-581 (2003).
57. Cserr, H.F. & Knopf, P.M. Cervical lymphatics, the blood-brain barrier and the immunoreactivity of the brain: a new view. *Immunol Today* **13**, 507-512 (1992).
58. Bartholomaus, I., *et al.* Effector T cell interactions with meningeal vascular structures in nascent autoimmune CNS lesions. *Nature* **462**, 94-98 (2009).
59. Goverman, J. Autoimmune T cell responses in the central nervous system. *Nat Rev Immunol* **9**, 393-407 (2009).
60. Scherer, S.S. & Wrabetz, L. Molecular mechanisms of inherited demyelinating neuropathies. *Glia* **56**, 1578-1589 (2008).
61. Bunge, M.B., Bunge, R.P. & Pappas, G.D. Electron microscopic demonstration of connections between glia and myelin sheaths in the developing mammalian central nervous system. *J Cell Biol* **12**, 448-453 (1962).
62. Zalc, B., Goujet, D. & Colman, D. The origin of the myelination program in vertebrates. *Curr Biol* **18**, R511-512 (2008).
63. Nave, K.A. Myelination and the trophic support of long axons. *Nat Rev Neurosci* **11**, 275-283 (2010).
64. Remahl, S. & Hildebrand, C. Changing relation between onset of myelination and axon diameter range in developing feline white matter. *J Neurol Sci* **54**, 33-45 (1982).

65. Arroyo, E.J. & Scherer, S.S. On the molecular architecture of myelinated fibers. *Histochem Cell Biol* **113**, 1-18 (2000).
66. Butt, A.M. & Ransom, B.R. Visualization of oligodendrocytes and astrocytes in the intact rat optic nerve by intracellular injection of lucifer yellow and horseradish peroxidase. *Glia* **2**, 470-475 (1989).
67. Poliak, S. & Peles, E. The local differentiation of myelinated axons at nodes of Ranvier. *Nat Rev Neurosci* **4**, 968-980 (2003).
68. Larocca, J.N. & Rodriguez-Gabin, A.G. Myelin biogenesis: vesicle transport in oligodendrocytes. *Neurochem Res* **27**, 1313-1329 (2002).
69. Geren, B.B. & Raskind, J. Development of the Fine Structure of the Myelin Sheath in Sciatic Nerves of Chick Embryos. *Proc Natl Acad Sci U S A* **39**, 880-884 (1953).
70. Lemke, G. Unwrapping myelination. *Nature* **383**, 395-396 (1996).
71. Hirano, A. & Dembitzer, H.M. A structural analysis of the myelin sheath in the central nervous system. *J Cell Biol* **34**, 555-567 (1967).
72. Inoue, Y., Nakamura, R., Mikoshiba, K. & Tsukada, Y. Fine structure of the central myelin sheath in the myelin deficient mutant Shiverer mouse, with special reference to the pattern of myelin formation by oligodendroglia. *Brain Res* **219**, 85-94 (1981).
73. Readhead, C., *et al.* Expression of a myelin basic protein gene in transgenic shiverer mice: correction of the dysmyelinating phenotype. *Cell* **48**, 703-712 (1987).
74. Willard, H.F. & Riordan, J.R. Assignment of the gene for myelin proteolipid protein to the X chromosome: implications for X-linked myelin disorders. *Science* **230**, 940-942 (1985).
75. Sidman, R.L., Dickie, M.M. & Appel, S.H. Mutant Mice (Quaking and Jimpy) with Deficient Myelination in the Central Nervous System. *Science* **144**, 309-311 (1964).
76. Duncan, I.D., Hammang, J.P., Goda, S. & Quarles, R.H. Myelination in the jimpy mouse in the absence of proteolipid protein. *Glia* **2**, 148-154 (1989).
77. Klugmann, M., *et al.* Assembly of CNS myelin in the absence of proteolipid protein. *Neuron* **18**, 59-70 (1997).
78. Saher, G., *et al.* High cholesterol level is essential for myelin membrane growth. *Nat Neurosci* **8**, 468-475 (2005).
79. Inoue, K. PLP1-related inherited dysmyelinating disorders: Pelizaeus-Merzbacher disease and spastic paraplegia type 2. *Neurogenetics* **6**, 1-16 (2005).
80. Brockschnieder, D., Sabanay, H., Riethmacher, D. & Peles, E. Ermin, a myelinating oligodendrocyte-specific protein that regulates cell morphology. *J Neurosci* **26**, 757-762 (2006).
81. Peters, A. A radial component of central myelin sheaths. *J Biophys Biochem Cytol* **11**, 733-735 (1961).
82. Morita, K., Sasaki, H., Fujimoto, K., Furuse, M. & Tsukita, S. Claudin-11/OSP-based tight junctions of myelin sheaths in brain and Sertoli cells in testis. *J Cell Biol* **145**, 579-588 (1999).
83. Bronstein, J.M., Micevych, P.E. & Chen, K. Oligodendrocyte-specific protein (OSP) is a major component of CNS myelin. *J Neurosci Res* **50**, 713-720 (1997).
84. Gow, A., *et al.* CNS myelin and sertoli cell tight junction strands are absent in Osp/claudin-11 null mice. *Cell* **99**, 649-659 (1999).
85. Gollan, L., Salomon, D., Salzer, J.L. & Peles, E. Caspr regulates the processing of contactin and inhibits its binding to neurofascin. *J Cell Biol* **163**, 1213-1218 (2003).

86. Sherman, D.L., *et al.* Neurofascins are required to establish axonal domains for saltatory conduction. *Neuron* **48**, 737-742 (2005).
87. Boyle, M.E., *et al.* Contactin orchestrates assembly of the septate-like junctions at the paranode in myelinated peripheral nerve. *Neuron* **30**, 385-397 (2001).
88. Bunge, R.P., Bunge, M.B. & Bates, M. Movements of the Schwann cell nucleus implicate progression of the inner (axon-related) Schwann cell process during myelination. *J Cell Biol* **109**, 273-284 (1989).
89. Ben Geren, B. The formation from the Schwann cell surface of myelin in the peripheral nerves of chick embryos. *Exp Cell Res* **7**, 558-562 (1954).
90. Luse, S.A. Formation of myelin in the central nervous system of mice and rats, as studied with the electron microscope. *J Biophys Biochem Cytol* **2**, 777-784 (1956).
91. De Robertis, E., Gerschenfeld, H.M. & Wald, F. Cellular mechanism of myelination in the central nervous system. *J Biophys Biochem Cytol* **4**, 651-656 (1958).
92. Peters, A. The formation and structure of myelin sheaths in the central nervous system. *J Biophys Biochem Cytol* **8**, 431-446 (1960).
93. Bunge, M.B., Bunge, R.P. & Ris, H. Ultrastructural study of remyelination in an experimental lesion in adult cat spinal cord. *J Biophys Biochem Cytol* **10**, 67-94 (1961).
94. Webster, H.D. The geometry of peripheral myelin sheaths during their formation and growth in rat sciatic nerves. *J Cell Biol* **48**, 348-367 (1971).
95. Knobler, R.L., Stempak, J.G. & Laurencin, M. Nonuniformity of the oligodendroglial ensheathment of axons during myelination in the developing rat central nervous system. A serial section electron microscopical study. *J Ultrastruct Res* **55**, 417-432 (1976).
96. Fraher, J.P. Quantitative studies on the maturation of central and peripheral parts of individual ventral motoneuron axons. I. Myelin sheath and axon calibre. *J Anat* **126**, 509-533 (1978).
97. Berry, M., *et al.* Axon-glial relationships in the anterior medullary velum of the adult rat. *J Neurocytol* **24**, 965-983 (1995).
98. Pedraza, L., Huang, J.K. & Colman, D. Disposition of axonal caspr with respect to glial cell membranes: Implications for the process of myelination. *J Neurosci Res* **87**, 3480-3491 (2009).
99. Arroyo, E.J., *et al.* Myelinating Schwann cells determine the internodal localization of Kv1.1, Kv1.2, Kvbeta2, and Caspr. *J Neurocytol* **28**, 333-347 (1999).
100. Hildebrand, C., Remahl, S., Persson, H. & Bjartmar, C. Myelinated nerve fibres in the CNS. *Prog Neurobiol* **40**, 319-384 (1993).
101. Bauer, N.G., Richter-Landsberg, C. & Ffrench-Constant, C. Role of the oligodendroglial cytoskeleton in differentiation and myelination. *Glia* **57**, 1691-1705 (2009).
102. Spassky, N., *et al.* Multiple restricted origin of oligodendrocytes. *J Neurosci* **18**, 8331-8343 (1998).
103. Cao, Y., *et al.* Induction of experimental autoimmune encephalomyelitis in transgenic mice expressing ovalbumin in oligodendrocytes. *Eur J Immunol* **36**, 207-215 (2006).
104. Wight, P.A., Duchala, C.S., Readhead, C. & Macklin, W.B. A myelin proteolipid protein-LacZ fusion protein is developmentally regulated and targeted to the myelin membrane in transgenic mice. *J Cell Biol* **123**, 443-454 (1993).
105. Gahwiler, B.H., Capogna, M., Debanne, D., McKinney, R.A. & Thompson, S.M. Organotypic slice cultures: a technique has come of age. *Trends Neurosci* **20**, 471-477 (1997).

106. Stoppini, L., Buchs, P.A. & Muller, D. A simple method for organotypic cultures of nervous tissue. *J Neurosci Methods* **37**, 173-182 (1991).
107. Garcia, K.C., Teyton, L. & Wilson, I.A. Structural basis of T cell recognition. *Annu Rev Immunol* **17**, 369-397 (1999).
108. Kawakami, N., *et al.* Live imaging of effector cell trafficking and autoantigen recognition within the unfolding autoimmune encephalomyelitis lesion. *J Exp Med* **201**, 1805-1814 (2005).
109. Sobottka, B., *et al.* Collateral bystander damage by myelin-directed CD8+ T cells causes axonal loss. *Am J Pathol* **175**, 1160-1166 (2009).
110. Davidson, A. & Diamond, B. Autoimmune diseases. *N Engl J Med* **345**, 340-350 (2001).
111. Sriram, S. & Steiner, I. Experimental allergic encephalomyelitis: a misleading model of multiple sclerosis. *Ann Neurol* **58**, 939-945 (2005).
112. Friese, M.A. & Fugger, L. Pathogenic CD8(+) T cells in multiple sclerosis. *Ann Neurol* **66**, 132-141 (2009).
113. Wucherpfennig, K.W., *et al.* T cell receptor V alpha-V beta repertoire and cytokine gene expression in active multiple sclerosis lesions. *J Exp Med* **175**, 993-1002 (1992).
114. Booss, J., Esiri, M.M., Tourtellotte, W.W. & Mason, D.Y. Immunohistological analysis of T lymphocyte subsets in the central nervous system in chronic progressive multiple sclerosis. *J Neurol Sci* **62**, 219-232 (1983).
115. Jacobsen, M., *et al.* Oligoclonal expansion of memory CD8+ T cells in cerebrospinal fluid from multiple sclerosis patients. *Brain* **125**, 538-550 (2002).
116. Zang, Y.C., *et al.* Increased CD8+ cytotoxic T cell responses to myelin basic protein in multiple sclerosis. *J Immunol* **172**, 5120-5127 (2004).
117. Kuhlmann, T., Lingfeld, G., Bitsch, A., Schuchardt, J. & Bruck, W. Acute axonal damage in multiple sclerosis is most extensive in early disease stages and decreases over time. *Brain* **125**, 2202-2212 (2002).
118. Hoftberger, R., *et al.* Expression of major histocompatibility complex class I molecules on the different cell types in multiple sclerosis lesions. *Brain Pathol* **14**, 43-50 (2004).
119. Huseby, E.S., Ohlen, C. & Goverman, J. Cutting edge: myelin basic protein-specific cytotoxic T cell tolerance is maintained in vivo by a single dominant epitope in H-2k mice. *J Immunol* **163**, 1115-1118 (1999).
120. Morgan, D.J., *et al.* CD8(+) T cell-mediated spontaneous diabetes in neonatal mice. *J Immunol* **157**, 978-983 (1996).
121. Galea, I., *et al.* An antigen-specific pathway for CD8 T cells across the blood-brain barrier. *J Exp Med* **204**, 2023-2030 (2007).
122. Engelhardt, B. & Ransohoff, R.M. The ins and outs of T-lymphocyte trafficking to the CNS: anatomical sites and molecular mechanisms. *Trends Immunol* **26**, 485-495 (2005).
123. Hovelmeyer, N., *et al.* Apoptosis of oligodendrocytes via Fas and TNF-R1 is a key event in the induction of experimental autoimmune encephalomyelitis. *J Immunol* **175**, 5875-5884 (2005).
124. Gobel, K., *et al.* Collateral neuronal apoptosis in CNS gray matter during an oligodendrocyte-directed CD8(+) T cell attack. *Glia* **58**, 469-480 (2010).
125. Townsend, A.R., *et al.* The epitopes of influenza nucleoprotein recognized by cytotoxic T lymphocytes can be defined with short synthetic peptides. *Cell* **44**, 959-968 (1986).
126. Suzumura, A., Lavi, E., Weiss, S.R. & Silberberg, D.H. Coronavirus infection induces H-2 antigen expression on oligodendrocytes and astrocytes. *Science* **232**, 991-993 (1986).

127. Redwine, J.M., Buchmeier, M.J. & Evans, C.F. In vivo expression of major histocompatibility complex molecules on oligodendrocytes and neurons during viral infection. *Am J Pathol* **159**, 1219-1224 (2001).
128. Neumann, H., Cavalie, A., Jenne, D.E. & Wekerle, H. Induction of MHC class I genes in neurons. *Science* **269**, 549-552 (1995).
129. Sensenbrenner, M., Lucas, M. & Deloulme, J.C. Expression of two neuronal markers, growth-associated protein 43 and neuron-specific enolase, in rat glial cells. *J Mol Med* **75**, 653-663 (1997).
130. Grimm, E.A., Mazumder, A., Zhang, H.Z. & Rosenberg, S.A. Lymphokine-activated killer cell phenomenon. Lysis of natural killer-resistant fresh solid tumor cells by interleukin 2-activated autologous human peripheral blood lymphocytes. *J Exp Med* **155**, 1823-1841 (1982).
131. Vergelli, M., *et al.* A novel population of CD4+CD56+ myelin-reactive T cells lyses target cells expressing CD56/neural cell adhesion molecule. *J Immunol* **157**, 679-688 (1996).
132. Knickelbein, J.E., *et al.* Noncytotoxic lytic granule-mediated CD8+ T cell inhibition of HSV-1 reactivation from neuronal latency. *Science* **322**, 268-271 (2008).
133. Kim, J.V., Kang, S.S., Dustin, M.L. & McGavern, D.B. Myelomonocytic cell recruitment causes fatal CNS vascular injury during acute viral meningitis. *Nature* **457**, 191-195 (2009).
134. Dustin, M.L. & Long, E.O. Cytotoxic immunological synapses. *Immunol Rev* **235**, 24-34 (2010).
135. Faroudi, M., *et al.* Lytic versus stimulatory synapse in cytotoxic T lymphocyte/target cell interaction: manifestation of a dual activation threshold. *Proc Natl Acad Sci U S A* **100**, 14145-14150 (2003).
136. Jenkins, M.R., Tsun, A., Stinchcombe, J.C. & Griffiths, G.M. The strength of T cell receptor signal controls the polarization of cytotoxic machinery to the immunological synapse. *Immunity* **31**, 621-631 (2009).
137. Harrer, M.D., *et al.* Live imaging of remyelination after antibody-mediated demyelination in an ex-vivo model for immune mediated CNS damage. *Exp Neurol* (2009).
138. Kelly, J.M., *et al.* Identification of conserved T cell receptor CDR3 residues contacting known exposed peptide side chains from a major histocompatibility complex class I-bound determinant. *Eur J Immunol* **23**, 3318-3326 (1993).
139. Hogquist, K.A., *et al.* T cell receptor antagonist peptides induce positive selection. *Cell* **76**, 17-27 (1994).
140. Clarke, S.R., *et al.* Characterization of the ovalbumin-specific TCR transgenic line OT-I: MHC elements for positive and negative selection. *Immunol Cell Biol* **78**, 110-117 (2000).
141. Taveggia, C., Feltri, M.L. & Wrabetz, L. Signals to promote myelin formation and repair. *Nat Rev Neurol* **6**, 276-287 (2010).
142. Piaton, G., Gould, R.M. & Lubetzki, C. Axon-oligodendrocyte interactions during developmental myelination, demyelination and repair. *J Neurochem* **114**, 1243-1260 (2010).

143. Aguayo, A.J., Charron, L. & Bray, G.M. Potential of Schwann cells from unmyelinated nerves to produce myelin: a quantitative ultrastructural and radiographic study. *J Neurocytol* **5**, 565-573 (1976).
144. Dubois-Dalcq, M., Behar, T., Hudson, L. & Lazzarini, R.A. Emergence of three myelin proteins in oligodendrocytes cultured without neurons. *J Cell Biol* **102**, 384-392 (1986).
145. Friede, R.L. Control of myelin formation by axon caliber (with a model of the control mechanism). *J Comp Neurol* **144**, 233-252 (1972).
146. Fanarraga, M.L., Griffiths, I.R., Zhao, M. & Duncan, I.D. Oligodendrocytes are not inherently programmed to myelinate a specific size of axon. *J Comp Neurol* **399**, 94-100 (1998).
147. Elder, G.A., Friedrich, V.L., Jr. & Lazzarini, R.A. Schwann cells and oligodendrocytes read distinct signals in establishing myelin sheath thickness. *J Neurosci Res* **65**, 493-499 (2001).
148. Setzu, A., Ffrench-Constant, C. & Franklin, R.J. CNS axons retain their competence for myelination throughout life. *Glia* **45**, 307-311 (2004).
149. Lubetzki, C., *et al.* Even in culture, oligodendrocytes myelinate solely axons. *Proc Natl Acad Sci U S A* **90**, 6820-6824 (1993).
150. Taveggia, C., *et al.* Neuregulin-1 type III determines the ensheathment fate of axons. *Neuron* **47**, 681-694 (2005).
151. Michailov, G.V., *et al.* Axonal neuregulin-1 regulates myelin sheath thickness. *Science* **304**, 700-703 (2004).
152. Brinkmann, B.G., *et al.* Neuregulin-1/ErbB signaling serves distinct functions in myelination of the peripheral and central nervous system. *Neuron* **59**, 581-595 (2008).
153. Bremer, J., *et al.* Axonal prion protein is required for peripheral myelin maintenance. *Nat Neurosci* **13**, 310-318 (2010).
154. Buttery, P.C. & ffrench-Constant, C. Laminin-2/integrin interactions enhance myelin membrane formation by oligodendrocytes. *Mol Cell Neurosci* **14**, 199-212 (1999).
155. Chun, S.J., Rasband, M.N., Sidman, R.L., Habib, A.A. & Vartanian, T. Integrin-linked kinase is required for laminin-2-induced oligodendrocyte cell spreading and CNS myelination. *J Cell Biol* **163**, 397-408 (2003).
156. Jones, K.J., *et al.* The expanding phenotype of laminin alpha2 chain (merosin) abnormalities: case series and review. *J Med Genet* **38**, 649-657 (2001).
157. Relvas, J.B., *et al.* Expression of dominant-negative and chimeric subunits reveals an essential role for beta1 integrin during myelination. *Curr Biol* **11**, 1039-1043 (2001).
158. Camara, J., *et al.* Integrin-mediated axoglial interactions initiate myelination in the central nervous system. *J Cell Biol* **185**, 699-712 (2009).
159. Laursen, L.S., Chan, C.W. & ffrench-Constant, C. An integrin-contactin complex regulates CNS myelination by differential Fyn phosphorylation. *J Neurosci* **29**, 9174-9185 (2009).
160. Oumesmar, B.N., *et al.* Expression of the highly polysialylated neural cell adhesion molecule during postnatal myelination and following chemically induced demyelination of the adult mouse spinal cord. *Eur J Neurosci* **7**, 480-491 (1995).
161. Charles, P., *et al.* Negative regulation of central nervous system myelination by polysialylated-neural cell adhesion molecule. *Proc Natl Acad Sci U S A* **97**, 7585-7590 (2000).

162. Charles, P., *et al.* Re-expression of PSA-NCAM by demyelinated axons: an inhibitor of remyelination in multiple sclerosis? *Brain* **125**, 1972-1979 (2002).
163. Wang, S., *et al.* Notch receptor activation inhibits oligodendrocyte differentiation. *Neuron* **21**, 63-75 (1998).
164. Genoud, S., *et al.* Notch1 control of oligodendrocyte differentiation in the spinal cord. *J Cell Biol* **158**, 709-718 (2002).
165. Zhang, Y., *et al.* Notch1 signaling plays a role in regulating precursor differentiation during CNS remyelination. *Proc Natl Acad Sci U S A* **106**, 19162-19167 (2009).
166. Barry, C., Pearson, C. & Barbarese, E. Morphological organization of oligodendrocyte processes during development in culture and in vivo. *Dev Neurosci* **18**, 233-242 (1996).
167. Jones, D.P. Intracellular diffusion gradients of O2 and ATP. *Am J Physiol* **250**, C663-675 (1986).
168. Corriden, R. & Insel, P.A. Basal release of ATP: an autocrine-paracrine mechanism for cell regulation. *Sci Signal* **3**, re1 (2010).
169. Rosenberg, S.S., Kelland, E.E., Tokar, E., De la Torre, A.R. & Chan, J.R. The geometric and spatial constraints of the microenvironment induce oligodendrocyte differentiation. *Proc Natl Acad Sci U S A* **105**, 14662-14667 (2008).
170. Szuchet, S., Polak, P.E. & Yim, S.H. Mature oligodendrocytes cultured in the absence of neurons recapitulate the ontogenic development of myelin membranes. *Dev Neurosci* **8**, 208-221 (1986).
171. Althaus, H.H., Montz, H., Neuhoff, V. & Schwartz, P. Isolation and cultivation of mature oligodendroglial cells. *Naturwissenschaften* **71**, 309-315 (1984).
172. Stevens, B., Porta, S., Haak, L.L., Gallo, V. & Fields, R.D. Adenosine: a neuron-glial transmitter promoting myelination in the CNS in response to action potentials. *Neuron* **36**, 855-868 (2002).
173. Demerens, C., *et al.* Induction of myelination in the central nervous system by electrical activity. *Proc Natl Acad Sci U S A* **93**, 9887-9892 (1996).
174. Kiryu-Seo, S., Ohno, N., Kidd, G.J., Komuro, H. & Trapp, B.D. Demyelination increases axonal stationary mitochondrial size and the speed of axonal mitochondrial transport. *J Neurosci* **30**, 6658-6666 (2010).
175. Hirokawa, N., Noda, Y., Tanaka, Y. & Niwa, S. Kinesin superfamily motor proteins and intracellular transport. *Nat Rev Mol Cell Biol* **10**, 682-696 (2009).
176. Zhao, C., *et al.* Charcot-Marie-Tooth disease type 2A caused by mutation in a microtubule motor KIF1Bbeta. *Cell* **105**, 587-597 (2001).
177. Aulchenko, Y.S., *et al.* Genetic variation in the KIF1B locus influences susceptibility to multiple sclerosis. *Nat Genet* **40**, 1402-1403 (2008).
178. Menegoz, M., *et al.* Paranodin, a glycoprotein of neuronal paranodal membranes. *Neuron* **19**, 319-331 (1997).
179. Einheber, S., *et al.* The axonal membrane protein Caspr, a homologue of neurexin IV, is a component of the septate-like paranodal junctions that assemble during myelination. *J Cell Biol* **139**, 1495-1506 (1997).
180. Tait, S., *et al.* An oligodendrocyte cell adhesion molecule at the site of assembly of the paranodal axo-glial junction. *J Cell Biol* **150**, 657-666 (2000).
181. Gollan, L., *et al.* Retention of a cell adhesion complex at the paranodal junction requires the cytoplasmic region of Caspr. *J Cell Biol* **157**, 1247-1256 (2002).

182. Bhat, M.A., *et al.* Axon-glia interactions and the domain organization of myelinated axons requires neurexin IV/Caspr/Paranodin. *Neuron* **30**, 369-383 (2001).
183. Felts, P.A., Baker, T.A. & Smith, K.J. Conduction in segmentally demyelinated mammalian central axons. *J Neurosci* **17**, 7267-7277 (1997).
184. Blakemore, W.F. Pattern of remyelination in the CNS. *Nature* **249**, 577-578 (1974).
185. Ludwin, S.K. & Maitland, M. Long-term remyelination fails to reconstitute normal thickness of central myelin sheaths. *J Neurol Sci* **64**, 193-198 (1984).
186. Blakemore, W.F. & Franklin, R.J. Remyelination in experimental models of toxin-induced demyelination. *Curr Top Microbiol Immunol* **318**, 193-212 (2008).
187. Xin, M., *et al.* Myelinogenesis and axonal recognition by oligodendrocytes in brain are uncoupled in Olig1-null mice. *J Neurosci* **25**, 1354-1365 (2005).
188. Stidworthy, M.F., *et al.* Notch1 and Jagged1 are expressed after CNS demyelination, but are not a major rate-determining factor during remyelination. *Brain* **127**, 1928-1941 (2004).
189. Stys, P.K., Waxman, S.G. & Ransom, B.R. Ionic mechanisms of anoxic injury in mammalian CNS white matter: role of Na+ channels and Na(+)-Ca2+ exchanger. *J Neurosci* **12**, 430-439 (1992).
190. Morfini, G.A., *et al.* Axonal transport defects in neurodegenerative diseases. *J Neurosci* **29**, 12776-12786 (2009).
191. Dutta, R., *et al.* Mitochondrial dysfunction as a cause of axonal degeneration in multiple sclerosis patients. *Ann Neurol* **59**, 478-489 (2006).
192. Mi, S., *et al.* LINGO-1 negatively regulates myelination by oligodendrocytes. *Nat Neurosci* **8**, 745-751 (2005).
193. Ffrench-Constant, C. & Raff, M.C. Proliferating bipotential glial progenitor cells in adult rat optic nerve. *Nature* **319**, 499-502 (1986).
194. Kirby, B.B., *et al.* In vivo time-lapse imaging shows dynamic oligodendrocyte progenitor behavior during zebrafish development. *Nat Neurosci* **9**, 1506-1511 (2006).
195. Gensert, J.M. & Goldman, J.E. Endogenous progenitors remyelinate demyelinated axons in the adult CNS. *Neuron* **19**, 197-203 (1997).
196. Arnett, H.A., *et al.* bHLH transcription factor Olig1 is required to repair demyelinated lesions in the CNS. *Science* **306**, 2111-2115 (2004).
197. Carroll, W.M., Jennings, A.R. & Ironside, L.J. Identification of the adult resting progenitor cell by autoradiographic tracking of oligodendrocyte precursors in experimental CNS demyelination. *Brain* **121 (Pt 2)**, 293-302 (1998).
198. Groves, A.K., *et al.* Repair of demyelinated lesions by transplantation of purified O-2A progenitor cells. *Nature* **362**, 453-455 (1993).
199. Nunes, M.C., *et al.* Identification and isolation of multipotential neural progenitor cells from the subcortical white matter of the adult human brain. *Nat Med* **9**, 439-447 (2003).
200. Levine, J.M. & Reynolds, R. Activation and proliferation of endogenous oligodendrocyte precursor cells during ethidium bromide-induced demyelination. *Exp Neurol* **160**, 333-347 (1999).
201. Sim, F.J., Zhao, C., Penderis, J. & Franklin, R.J. The age-related decrease in CNS remyelination efficiency is attributable to an impairment of both oligodendrocyte progenitor recruitment and differentiation. *J Neurosci* **22**, 2451-2459 (2002).

202. Targett, M.P., *et al.* Failure to achieve remyelination of demyelinated rat axons following transplantation of glial cells obtained from the adult human brain. *Neuropathol Appl Neurobiol* **22**, 199-206 (1996).
203. Keirstead, H.S. & Blakemore, W.F. Identification of post-mitotic oligodendrocytes incapable of remyelination within the demyelinated adult spinal cord. *J Neuropathol Exp Neurol* **56**, 1191-1201 (1997).